Analytical solutions for diffuse fluorescence spectroscopy/imaging in biological tissues. Part I: zero and extrapolated boundary conditions

Kalyan Ram Ayyalasomayajula and Phaneendra K. Yalavarthy*

Supercomputer Education and Research Centre, Indian Institute of Science, Bangalore 560 012, India
**Corresponding author: phani@serc.iisc.in*

Received December 11, 2012; accepted January 13, 2013;
posted January 16, 2013 (Doc. ID 181535); published February 28, 2013

The mathematical model for diffuse fluorescence spectroscopy/imaging is represented by coupled partial differential equations (PDEs), which describe the excitation and emission light propagation in soft biological tissues. The generic closed-form solutions for these coupled PDEs are derived in this work for the case of regular geometries using the Green's function approach using both zero and extrapolated boundary conditions. The specific solutions along with the typical data types, such as integrated intensity and the mean time of flight, for various regular geometries were also derived for both time- and frequency-domain cases.

OCIS codes: 170.0170, 170.6280, 300.2530, 000.3860.

1. INTRODUCTION

Fluorescence diffuse optical spectroscopy/imaging requires an exogenous drug to be injected into the tissue under investigation, which is excited by a near-infrared laser to emit the fluorescence light. The emitted fluorescence light is typically dependent on the lifetime and concentration of the exogenous drug coupled with physiology associated with the tissue under investigation [1,2]. The preferential uptake by the tumor vasculature leads to high contrast, making this modality one of the biggest contenders in small-animal and soft-tissue molecular imaging modalities [2].

As there is an excitation and emission of the light, the underlying physics of the problem is described by coupled diffusion equations [3]. These coupled diffusion equations are typically solved by advanced numerical methods, which tend to be computationally demanding. Similar to diffuse optical imaging [4–6], the aim of this work is to derive the analytical solution for these coupled partial differential equations (PDEs) for the simple geometries of both time-domain and frequency-domain cases. The existing literature [3,7–9] has not dealt with all simple geometries (more in the discussion section) and has derived analytical solutions for only a couple of geometries. Here a comprehensive discussion of all possible regular geometries and the corresponding time- and frequency-domain solutions are derived. These solutions can play an important role in determining the bulk fluorescence properties of the tissue, which could act as good initial guesses for the advanced image-reconstruction techniques and/or could also facilitate the calibration of experimental fluorescence data by removing biases and source-detector variations.

These solutions along with a detailed derivation of explicit forms for both zero and extrapolated boundary conditions are presented here. Importantly, this is the first time extrapolated boundary conditions (EBCs) are used in deriving analytical solutions for the fluorescence imaging. The existing closed-form solutions [3,7–9] have used only zero boundary conditions (ZBCs). A numerical comparison of these closed forms as well as a comparison with a well-established numerical model are taken up in the next part of this work [10]. This comparison not only validates the analytical expressions derived in this work, but also shows that the obtained results are in good agreement with the established numerical models.

2. DERIVATION OF ANALYTICAL SOLUTIONS FOR FLOURESCENCE OPTICAL SPECTROSCOPY/IMAGING

A. Coupled Diffusion Equations in Fluorescence Optical Spectroscopy/Imaging

We consider the basic equation of light transport in an isotropic medium and extend the principle equation of diffuse optical imaging to fluorescence optical spectroscopy/imaging as a two-stage system of excitation and emission. This leads to coupled differential equations in time-dependent and frequency-dependent cases as shown below.

Time-domain case:

$$\left[\gamma_x^2\nabla^2 - \mu_{ax}c - \frac{\partial}{\partial t}\right]\Phi_x(\mathbf{r},t) = -q_0(\mathbf{r},t), \tag{1}$$

$$\left[\gamma_m^2\nabla^2 - \mu_{am}c - \frac{\partial}{\partial t}\right]\Phi_m(\mathbf{r},t) = -q_{\mathrm{fl}}(\mathbf{r},t). \tag{2}$$

Table 1. Glossary of Notation of Symbols in the Equations Used in This Work

Symbol	Description (x Stands for Excitation, m Stands for Emission)
$\mu_{ax,am}(\mathbf{r})$	Absorption coefficient
$\mu'_{sx,sm}(\mathbf{r})$	Reduced scattering coefficient
$\mathbf{r}$	Spatial position
$\kappa_{x,m}(\mathbf{r})$	Diffusion coefficient $\frac{1}{3[\mu_{ax,am}(\mathbf{r})+3[\mu'_{sx,sm}(\mathbf{r})]}$
c	Velocity of light
$\gamma^2_{x,m}$	$c\kappa_{x,m}(\mathbf{r})$
$\Phi_{x,m}(\mathbf{r},t)$	Photon density
$\mathbf{k}$	Spatial frequency
k	Magnitude of $\mathbf{k}$
$q_0(\mathbf{r},t)$, $Q_0(\mathbf{k},\omega)$	Isotropic continuous-wave source term (excitation)
$q_{\mathrm{fl}}(\mathbf{r},t)$, $Q_{\mathrm{fl}}(\mathbf{k},\omega)$	Isotropic continuous-wave source term (emission)
τ	Fluorescence lifetime of the fluorophore
η	Fluorescence quantum yield (ratio of photons emitted to photons absorbed)
μ_{af}	Absorption extinction coefficient
$N(\mathbf{r})$	Concentration of fluorophore
$n(\mathbf{r})$	$\eta\mu_{af}N(\mathbf{r})$
ZBC	Zero boundary condition
EBC	Extrapolated boundary condition

Frequency-domain case:

$$-[k^2\gamma_x^2+\mu_{ax}c+j\omega]\Phi_x(\mathbf{k},\omega)=-Q_0(\mathbf{k},\omega), \tag{3}$$

$$-[k^2\gamma_m^2+\mu_{am}c+j\omega]\Phi_m(\mathbf{k},\omega)=-Q_{\mathrm{fl}}(\mathbf{k},\omega). \tag{4}$$

Please refer to Table 1 for a complete description of the symbols used in this work. The underlying physics of fluorescent diffuse photon density waves is discussed in detail in [3,7–9]. The source terms in the time-domain and frequency-domain cases are given by

$$\left(1+\tau\frac{\partial}{\partial t}\right)q_{\mathrm{fl}}(\mathbf{r},t)=\eta\mu_{af}N(\mathbf{r})\Phi_x(\mathbf{r},t), \tag{5}$$

$$Q_{\mathrm{fl}}(\mathbf{r},\omega)=\frac{\eta\mu_{af}N(\mathbf{r})}{1+j\omega\tau}\Phi_x(\mathbf{r},\omega)=\frac{n(\mathbf{r})}{1+j\omega\tau}\Phi_x(\mathbf{r},\omega). \tag{6}$$

The main aim of this work is to find analytical solutions to the coupled differential equations, Eqs. (1)–(4) for the regular geometries. We use the Green's function approach in obtaining the analytical solution for these coupled PDEs. The regular geometries that are considered in this work are infinite, semi-infinite, infinite slab, infinite cylinder, circle, and sphere. For completeness, both transmission and reflection cases of data-collection strategies were considered. The derivation of analytical forms in this work is divided into two sections, the first one being the usage of the ZBC [4,5] and the second one dealing with the EBC [6]. The EBC is more applicable for the real-time scenarios by taking into account the refractive-index mismatch at the tissue boundary [6]. However, deployment of the ZBC leads to the generic closed-form solutions seamlessly, which could be extended for other scenarios as well.

3. ZERO BOUNDARY CONDITION

We assume that the photon density (Φ_{fl}) in the interior part of the domain is a continuous function of x, y, z, and t; and the same also holds for the first differential coefficient with regard to t and for the first and second differential coefficients with regard to x, y, and z—subjected to the Dirichlet boundary condition

$$\Phi_{\mathrm{fl}}(\mathbf{r},\mathbf{r}',t,t')|_{\partial\Omega}=0, \tag{7}$$

where Φ_{fl} is contained in the volume Ω bounded by a surface $\partial\Omega$, and $\hat{n}$ is the outward surface normal. The dependency of Φ_{fl} on the boundary condition and its generalization using the Green's function have been discussed in detail in [9]. To summarize, the ZBC assumes there is no mismatch in the refractive index at the boundary of the tissue.

A. Case 1: Infinite Geometry

We derive the analytical solution for the infinite geometry from first principles [5] as indicated below. From Eqs. (1), (2), and (5), we have

$$\left[1+\tau\frac{\partial}{\partial t}\right]\left[\gamma_m^2\nabla^2-\mu_{am}c-\frac{\partial}{\partial t}\right]\left[\gamma_x^2\nabla^2-\mu_{ax}c-\frac{\partial}{\partial t}\right]\Phi_m(\mathbf{r},t)=n q_0(\mathbf{r},t). \tag{8}$$

Let $g_{\mathrm{inf}}^{\phi_{\mathrm{fl}}}(\mathbf{r},\mathbf{r}',t,t')$ represent the Green's function of Φ_m, which is the response of a delta function [i.e., $q_0(\mathbf{r},t)=\delta(\mathbf{r}-\mathbf{r}',t-t')$ an impulse source place at $\mathbf{r}'$ at time instant t'].

Taking the four-dimensional Fourier transform, where $t\to\omega$, $\mathbf{r}\to\mathbf{k}$, leads to

$$[1+j\tau\omega][-(k^2\gamma_m^2+\mu_{am}c+j\omega)][-(k^2\gamma_x^2+\mu_{ax}c+j\omega)]G_{\mathrm{inf}}^{\phi_{\mathrm{fl}}}(\mathbf{k},\mathbf{r}',\omega,t')=n\mathcal{F}[\delta(\mathbf{r}-\mathbf{r}',t-t')]=ne^{-j(\mathbf{k}.\mathbf{r}'+\omega t')} \tag{9}$$

with usage of inverse Fourier transform, and simplifying gives

$$g_{\mathrm{inf}}^{\phi_{\mathrm{fl}}}(\mathbf{r},\mathbf{r}',t,t')=\frac{1}{(2\pi)^4}\int\left[\int_{-\infty}^{\infty}\frac{ne^{j[\mathbf{k}.(\mathbf{r}-\mathbf{r}')+\omega(t-t')]}\mathrm{d}\omega}{(1+j\tau\omega)(k^2\gamma_m^2+\mu_{am}c+j\omega)(k^2\gamma_x^2+\mu_{ax}c+j\omega)}\right]d^3\mathbf{k}, \tag{10}$$

which is the Green's function for the infinite domain. The Fourier transform of the above Green's function gives a frequency-domain Green's function of Φ_m, written as

$$G_{\text{inf}}^{\phi_{\text{fl}}}(\mathbf{r},\mathbf{r}',\omega,t') = \frac{1}{\sqrt{2\pi}}\int_{-\infty}^{\infty} g_{\text{inf}}^{\phi_{\text{fl}}}(\mathbf{r},\mathbf{r}',t,t')e^{-j\omega t}\mathrm{d}t = \frac{1}{(2\pi)^{7/2}}\int \frac{ne^{j[\mathbf{k}.(\mathbf{r}-\mathbf{r}')-\omega t']}d^3\mathbf{k}}{(1+j\tau\omega)(k^2\gamma_m^2+\mu_{am}c+j\omega)(k^2\gamma_x^2+\mu_{ax}c+j\omega)}. \tag{11}$$

The above integration is achieved by converting the Cartesian coordinate system to a spherical polar coordinate system, i.e., $d^3\mathbf{k} \rightarrow k^2 \sin\theta dk d\theta d\phi$, with ranges of $\phi \rightarrow [0, 2\pi]$, $\theta \rightarrow [0, \pi]$, $k \rightarrow [0, \infty)$, respectively.

Evaluating the simple integration with respect to (w.r.t.) ϕ leads to

$$G_{\text{inf}}^{\phi_{\text{fl}}}(\mathbf{r},\mathbf{r}',\omega,t') = \frac{ne^{-j\omega t'}}{(2\pi)^{5/2}}\int_0^{\pi}\left[\int_0^{\infty}\frac{k^2e^{jk\rho\cos\theta}\sin\theta}{(1+j\tau\omega)(k^2\gamma_m^2+\mu_{am}c+j\omega)(k^2\gamma_x^2+\mu_{ax}c+j\omega)}\mathrm{d}k\right]\mathrm{d}\theta, \tag{12}$$

where $\rho = |\mathbf{r}-\mathbf{r}'|$. Now integrating w.r.t. θ gives rise to

$$G_{\text{inf}}^{\phi_{\text{fl}}}(\mathbf{r},\mathbf{r}',\omega,t') = \frac{ne^{-j\omega t'}}{(2\pi)^{5/2}j\rho}\int_0^{\infty}\frac{k(e^{-jk\rho}-e^{jk\rho})}{(1+j\tau\omega)(k^2\gamma_m^2+\mu_{am}c+j\omega)(k^2\gamma_x^2+\mu_{ax}c+j\omega)}\mathrm{d}k. \tag{13}$$

As the numerators and denominators of the above equation are even functions in k, one can extend the limits of integration from $(0, \infty)$ to $(-\infty, \infty)$, resulting in

$$G_{\text{inf}}^{\phi_{\text{fl}}}(\mathbf{r},\mathbf{r}',\omega,t') = \frac{ne^{-j\omega t'}}{(2\pi)^{5/2}j\rho}\frac{1}{2}\int_{-\infty}^{\infty}\frac{k(e^{-jk\rho}-e^{jk\rho})}{(1+j\tau\omega)(k^2\gamma_m^2+\mu_{am}c+j\omega)(k^2\gamma_x^2+\mu_{ax}c+j\omega)}\mathrm{d}k. \tag{14}$$

As both the exponents contribute same to the integral, making $k = -k$ leads to

$$G_{\text{inf}}^{\phi_{\text{fl}}}(\mathbf{r},\mathbf{r}',\omega,t') = -\frac{ne^{-j\omega t'}}{(2\pi)^{5/2}j\rho(1+j\tau\omega)}\int_{-\infty}^{\infty}\frac{ke^{jk\rho}}{(k^2\gamma_m^2+\mu_{am}c+j\omega)(k^2\gamma_x^2+\mu_{ax}c+j\omega)}\mathrm{d}k. \tag{15}$$

Factorizing the denominator gives rise to

$$G_{\text{inf}}^{\phi_{\text{fl}}}(\mathbf{r},\mathbf{r}',\omega,t') = \mathcal{A}\int_{-\infty}^{\infty}\frac{e^{jk\rho}}{2\gamma_m^2\gamma_x^2}\left[\frac{1}{k+j\alpha_{m+}}+\frac{1}{k+j\alpha_{m-}}\right]\left[\frac{1}{k+j\alpha_{x-}}-\frac{1}{k+j\alpha_{x+}}\right]\frac{\mathrm{d}k}{j(\alpha_{x+}-\alpha_{x-})}, \tag{16}$$

where

$$\mathcal{A} = -\frac{ne^{-j\omega t'}}{(2\pi)^{5/2}j\rho(1+j\tau\omega)}, \qquad \alpha_x^2 = \frac{\mu_{ax}c+j\omega}{\gamma_x^2} = A_x^2e^{j\beta_x},$$
$$A_x = \frac{[\mu_{ax}^2c^2+\omega^2]^{\frac{1}{4}}}{\gamma_x}, \qquad \tan\beta_x = \frac{\omega}{\mu_{ax}c}, \qquad \alpha_{x+} = A_xe^{j\frac{\beta_x}{2}}, \quad \text{and} \quad \alpha_{x-} = A_xe^{j\left(\frac{\beta_x}{2}+\pi\right)},$$
$$\alpha_m^2 = \frac{\mu_{am}c+j\omega}{\gamma_m^2} = A_m^2e^{j\beta_m}, \qquad A_m = \frac{[\mu_{am}^2c^2+\omega^2]^{\frac{1}{4}}}{\gamma_m}, \qquad \tan\beta_m = \frac{\omega}{\mu_{am}c},$$
$$\alpha_{m+} = A_me^{j\frac{\beta_m}{2}}, \quad \text{and} \quad \alpha_{m-} = A_me^{j\left(\frac{\beta_m}{2}+\pi\right)}.$$

The right-hand side (RHS) of Eq. (16) has four poles at $k = j\alpha_{x+}$, $k = j\alpha_{x-}$, $k = j\alpha_{m+}$, and $k = j\alpha_{m-}$ (graphically shown in Fig. 1), making Eq. (16) equivalent to

$$G_{\text{inf}}^{\phi_{\text{fl}}}(\mathbf{r},\mathbf{r}',\omega,t') = -\frac{e^{-j\omega t'}}{j\rho\gamma_x^2\gamma_m^2(2\pi)^{5/2}}\frac{n}{1+j\tau\omega}\int_{-\infty}^{\infty}\frac{ke^{jk\rho}\mathrm{d}k}{(k+j\alpha_{m+})(k+j\alpha_{m-})(k+j\alpha_{x+})(k+j\alpha_{x-})}. \tag{17}$$

Representing the numerators and denominators by $P(k)e^{jk\rho}$ and $Q(k)$, respectively, leads to

$$G^{\phi_{\mathrm{fl}}}_{\mathrm{inf}}(\mathbf{r},\mathbf{r}',\omega,t') = -\frac{e^{-j\omega t'}}{j\rho\gamma_x^2\gamma_m^2(2\pi)^{5/2}}\frac{n}{1+j\tau\omega}\int_{-\infty}^{\infty}\frac{P(k)}{Q(k)}e^{jk\rho}\mathrm{d}k, \quad \text{with } \deg(Q(k)) \geq \deg(P(k))+1. \tag{18}$$

Applying Jordan's lemma [11] for the integral alone gives rise to

$$\int_{-\infty}^{\infty}\frac{P(k)}{Q(k)}e^{jk\rho}\mathrm{d}k = 2\pi j\sum_{I[k]>0}\mathrm{Res}\left[\frac{P(k)}{Q(k)}e^{jk\rho}\right]. \tag{19}$$

$$\begin{aligned}
&= 2\pi j\left[\frac{e^{-\alpha_{x+}\rho}}{2j\alpha_{x+}}\frac{j\alpha_{x+}}{j^2(\alpha_{x+}+\alpha_{m+})(\alpha_{x+}+\alpha_{m-})} + \frac{e^{-\alpha_{m+}\rho}}{2j\alpha_{m+}}\frac{j\alpha_{m+}}{j^2(\alpha_{m+}+\alpha_{x+})(\alpha_{m+}+\alpha_{x-})}\right]\\
&= \frac{2\pi j}{2}\left[-\frac{e^{-\alpha_{x+}\rho}}{(\alpha_{x+}+\alpha_{m+})(\alpha_{x+}+\alpha_{m-})} + \frac{e^{-\alpha_{m+}\rho}}{(\alpha_{m+}+\alpha_{x+})(\alpha_{x+}+\alpha_{m-})}\right] \quad \text{as } \alpha_{x+,m+} = -\alpha_{x-,m-}\\
&= -\frac{2\pi j}{2}\left[\frac{e^{-\alpha_{x+}\rho}-e^{-\alpha_{m+}\rho}}{\alpha_x^2-\alpha_m^2}\right] \quad \text{as } \alpha^2_{x+,m+} = \alpha^2_{x,m}
\end{aligned} \tag{20}$$

Substituting Eq. (20) in Eq. (18) results in

$$G^{\phi_{\mathrm{fl}}}_{\mathrm{inf}}(\mathbf{r},\mathbf{r}',\omega,t') = \left[-\frac{e^{-j\omega t'}}{\rho\gamma_x^2\gamma_m^2(2\pi)^{3/2}2\pi j}\frac{n}{(1+j\tau\omega)}\right]\left[-\frac{2\pi j}{2}\frac{(e^{-\alpha_{x+}\rho}-e^{-\alpha_{m+}\rho})}{\alpha_x^2-\alpha_m^2}\right],\ \omega>0, \tag{21}$$

$$G^{\phi_{\mathrm{fl}}}_{\mathrm{inf}}(\mathbf{r},\mathbf{r}',\omega,t') = \frac{ne^{-j\omega t'}}{2(2\pi)^{3/2}\rho\gamma_x^2\gamma_m^2}\frac{1}{(1+j\tau\omega)}\frac{(e^{-\alpha_x\rho}-e^{-\alpha_m\rho})}{\alpha_x^2-\alpha_m^2} \quad \text{where } \alpha_{x,m} = \frac{\sqrt{\mu_{ax,am}c+j\omega}}{\gamma_{x,m}}. \tag{22}$$

Expansion of terms gives

$$\begin{aligned}
G^{\phi_{\mathrm{fl}}}_{\mathrm{inf}}(\mathbf{r},\mathbf{r}',\omega,t') &= \frac{ne^{-j\omega t'}}{2(2\pi)^{3/2}\rho}(e^{-\alpha_x\rho}-e^{-\alpha_m\rho})\frac{1}{(1+j\tau\omega)[\gamma_m^2(\gamma_x^2\alpha_x^2)-\gamma_x^2(\gamma_m^2\alpha_m^2)]}\\
&= \frac{ne^{-j\omega t'}}{2(2\pi)^{3/2}\rho}\frac{(e^{-\alpha_x\rho}-e^{-\alpha_m\rho})}{(1+j\tau\omega)[\gamma_m^2(\mu_{ax}c+j\omega)-\gamma_x^2(\mu_{am}c+j\omega)]}\\
&= \frac{ne^{-j\omega t'}}{2(2\pi)^{3/2}\rho}\frac{(e^{-\alpha_x\rho}-e^{-\alpha_m\rho})}{(1+j\tau\omega)[\gamma_m^2\mu_{ax}c-\gamma_x^2\mu_{am}c+j(\gamma_m^2-\gamma_x^2)\omega]}\\
&= \frac{ne^{-j\omega t'}}{2(2\pi)^{3/2}\rho}\frac{(e^{-\alpha_x\rho}-e^{-\alpha_m\rho})}{(1+j\tau\omega)(\gamma_m^2\mu_{ax}c-\gamma_x^2\mu_{am}c)\left[1+j\frac{(\gamma_m^2-\gamma_x^2)}{(\gamma_m^2\mu_{ax}c-\gamma_x^2\mu_{am}c)}\omega\right]}\\
&= \frac{ne^{-j\omega t'}}{2(2\pi)^{3/2}\rho}\frac{(e^{-\alpha_x\rho}-e^{-\alpha_m\rho})}{\gamma_m^2-\gamma_x^2}\zeta^2\left[\frac{1}{1+j\tau\omega}\frac{1}{1+j\zeta^2\omega}\right] \quad \text{where } \zeta^2 = \frac{(\gamma_m^2-\gamma_x^2)}{(\gamma_m^2\mu_{ax}c-\gamma_x^2\mu_{am}c)}\\
&= \frac{ne^{-j\omega t'}}{2(2\pi)^{3/2}\rho}\frac{(e^{-\alpha_x\rho}-e^{-\alpha_m\rho})}{\gamma_m^2-\gamma_x^2}\zeta^2\left[\frac{1}{\tau-\zeta^2}\left\{\frac{\tau}{1+j\tau\omega}-\frac{\zeta^2}{1+j\zeta^2\omega}\right\}\right].
\end{aligned} \tag{23}$$

$G^{\phi_{\mathrm{fl}}}_{\mathrm{inf}}(\mathbf{r},\mathbf{r}',\omega,t')$ can be rearranged to give the analytical Green's function solution for the infinite domain case in the frequency domain as

$$G^{\phi_{\mathrm{fl}}}_{\mathrm{inf}}(\mathbf{r},\mathbf{r}',\omega,t') = \frac{n\zeta^2e^{-j\omega t'}}{(\gamma_m^2-\gamma_x^2)}\left[\frac{e^{-\alpha_x\rho}}{2\rho(2\pi)^{3/2}}-\frac{e^{-\alpha_m\rho}}{2\rho(2\pi)^{3/2}}\right]\cdot\left[\frac{1}{\tau-\zeta^2}\left\{\frac{1}{\frac{1}{\tau}+j\omega}-\frac{1}{\frac{1}{\zeta^2}+j\omega}\right\}\right]. \tag{24}$$

Multiplication in the frequency domain means convolution in the time domain, so the time-domain counterpart of the Green's function solution becomes

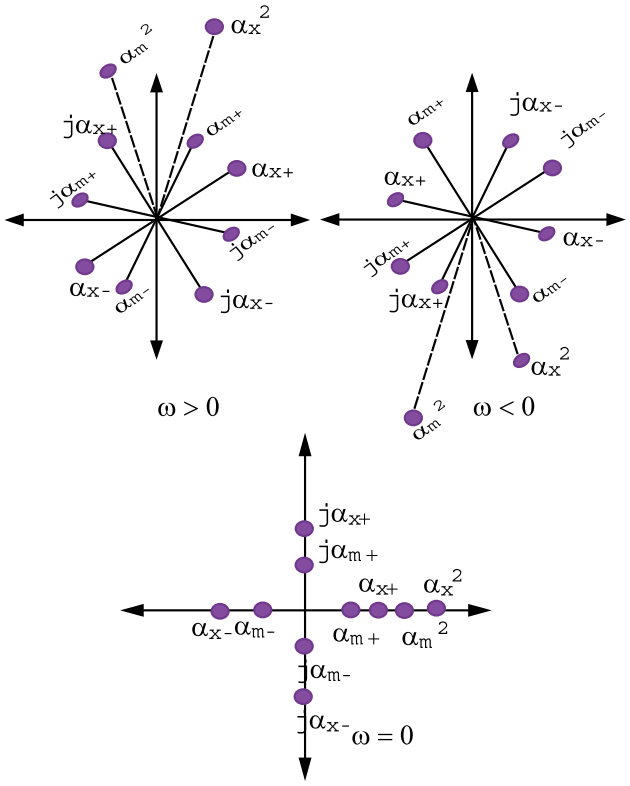

Fig. 1. (Color online) Plots indicating the position of poles with varying frequency for $\omega > 0$, $\omega < 0$, and $\omega = 0$ for the case of infinite geometry.

$$\therefore g_{\text{inf}}^{\phi_{\text{fl}}}(\mathbf{r},\mathbf{r}',t,t') = \frac{n\zeta^2}{(\gamma_m^2-\gamma_x^2)}[\gamma_x^2 g_{\text{inf}}^{\phi_x}(\mathbf{r},\mathbf{r}',t,t') - \gamma_m^2 g_{\text{inf}}^{\phi_m}(\mathbf{r},\mathbf{r}',t,t')] * \left[\frac{1}{\tau-\zeta^2}\left[\left(e^{-\frac{t}{\tau}} - e^{-\frac{t}{\zeta^2}}\right)u(t)\right]\right], \quad (25)$$

where

$$g_{\text{inf}}^{\phi_{x,m}}(\mathbf{r},\mathbf{r}',t,t') = \frac{1}{[4\pi\gamma_{x,m}^2(t-t')]^{3/2}} e^{-\left[\mu_{ax,am}c(t-t') + \frac{|\mathbf{r}-\mathbf{r}'|^2}{4\gamma_{x,m}^2(t-t')}\right]}. \quad (26)$$

$u(t)$ is the Heaviside step function.

B. Case 2: Semi-Infinite Geometry

Figure 2 shows an illustration of the imaging geometry used for derivation of the Green's function of $\phi(\rho,z,t)$ for a semi-infinite and infinite slab homogeneous medium. The incident pencil beam is assumed to create an isotropic photon source at a depth $z_0 = 1/(\mu_{sx}')$, indicated by the filled circle. The boundary condition $\phi(\rho,0,t) = 0$ can be achieved by adding a negative source indicated by the open circle [4], as shown in Fig. 2. Assuming an impulse source as in the earlier case results in [5,12],

$$g_{\text{half}}^{\phi}(\mathbf{r},\mathbf{r}',t,t') = \underbrace{\frac{1}{[4\pi\gamma^2(t-t')]^{3/2}} e^{-\left[\mu_a c(t-t') + \frac{|\mathbf{r}-\mathbf{r}'|^2}{4\gamma^2(t-t')}\right]}}_{g_{\text{inf}}^{\phi}(\mathbf{r},\mathbf{r}',t,t')} \times \left[e^{-\frac{(z-z_0)^2}{4\gamma^2(t-t')}} - e^{-\frac{(z+z_0)^2}{4\gamma^2(t-t')}}\right]. \quad (27)$$

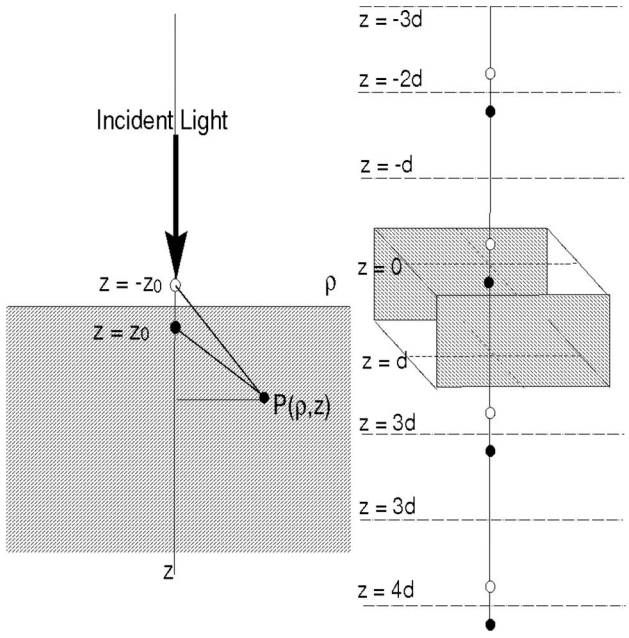

Fig. 2. Geometry indicating the source and detector distribution for semi-infinite domain (left) and infinite slab (right).

We observe that $g_{\text{half}}^{\phi}(\mathbf{r},\mathbf{r}',t,t') = g_{\text{inf}}^{\phi}(\mathbf{r},\mathbf{r}',t,t')[e^{-(z-z_0)^2/(4\gamma^2(t-t'))} - e^{-((z+z_0)^2/(4\gamma^2(t-t')))}]$; in other words, the Green's function solution of semi-infinite geometry is the Green's function solution of infinite geometry with two sources located at $+z_0$ and $-z_0$.

We make the following observations in the Green's function for the infinite case [9]:

$$g_{\text{inf}}^{\phi_{\text{fl}}}(\mathbf{r},\mathbf{r}',t,t') = \mathcal{C}\left[\underbrace{\gamma_x^2 g_{\text{inf}}^{\phi_x}(\mathbf{r},\mathbf{r}',t,t')}_{\text{SOURCE-1}} - \underbrace{\gamma_m^2 g_{\text{inf}}^{\phi_m}(\mathbf{r},\mathbf{r}',t,t')}_{\text{SOURCE-2}}\right] * \underbrace{\left[\frac{1}{\tau-\zeta^2}\left[\left(e^{-\frac{t}{\tau}} - e^{-\frac{t}{\zeta^2}}\right)u(t)\right]\right]}_{\text{SYSTEM}}, \quad (28)$$

where $\mathcal{C} = (n\zeta^2)/(\gamma_m^2 - \gamma_x^2)$.

The principle of superposition, which is valid for the linear system theory, can be extended to the semi-infinite case by considering the Green's function for the infinite geometry as a response to the system $1/(\tau-\zeta^2)[(e^{-(t/\tau)} - e^{-(t/\zeta^2)})u(t)]$ with inputs as $\gamma_x^2 g_{\text{inf}}^{\phi_x}(\mathbf{r},\mathbf{r}',t,t')$ and $\gamma_m^2 g_{\text{inf}}^{\phi_m}(\mathbf{r},\mathbf{r}',t,t')$. Now to arrive at an expression for the semi-infinite case these two source terms can be altered w.r.t. the spatial vector variable as shown in Eq. (27), leading to

$$\therefore g_{\text{half}}^{\phi_{\text{fl}}}(\mathbf{r},\mathbf{r}',t,t') = \frac{n\zeta^2}{(\gamma_m^2-\gamma_x^2)}[\gamma_x^2 g_{\text{half}}^{\phi_x}(\mathbf{r},\mathbf{r}',t,t') - \gamma_m^2 g_{\text{half}}^{\phi_m}(\mathbf{r},\mathbf{r}',t,t')] * \left[\frac{1}{\tau-\zeta^2}\left[\left(e^{-\frac{t}{\tau}} - e^{-\frac{t}{\zeta^2}}\right)u(t)\right]\right], \quad (29)$$

where

$$g^{\phi_{x,m}}_{\text{half}}(\mathbf{r},\mathbf{r}',t,t') = \frac{1}{[4\pi\gamma^2_{x,m}(t-t')]^{3/2}} e^{-\left[\mu_{ax,am}c(t-t')+\frac{|\mathbf{r}-\mathbf{r}'|^2}{4\gamma^2_{x,m}(t-t')}\right]} \times \left[e^{-\frac{(z-z_0)^2}{4\gamma^2_{x,m}(t-t')}} - e^{-\frac{(z+z_0)^2}{4\gamma^2_{x,m}(t-t')}}\right]. \quad (30)$$

By similar argument we can deduce the Green's function for the infinite slab case as [5,12]

$$g^{\phi_{\text{fl}}}_{\text{slab}}(\mathbf{r},\mathbf{r}',t,t') = \frac{n\zeta^2}{(\gamma_m^2-\gamma_x^2)}[\gamma_x^2 g^{\phi_x}_{\text{slab}}(\mathbf{r},\mathbf{r}',t,t') - \gamma_m^2 g^{\phi_m}_{\text{slab}}(\mathbf{r},\mathbf{r}',t,t')] * \left[\frac{1}{\tau-\zeta^2}\left[\left(e^{-\frac{t}{\tau}} - e^{-\frac{t}{\zeta^2}}\right)u(t)\right]\right], \quad (31)$$

where

$$g^{\phi_{x,m}}_{\text{slab}}(\mathbf{r},\mathbf{r}',t,t') = \frac{1}{[4\pi\gamma^2_{x,m}(t-t')]^{3/2}} e^{-\left[\mu_{ax,am}c(t-t')+\frac{|\mathbf{r}-\mathbf{r}'|^2}{4\gamma^2_{x,m}(t-t')}\right]} \times \left[\sum_{n=-\infty}^{\infty}\left(e^{-\frac{(z-2nd-z_0)^2}{4\gamma^2_{x,m}(t-t')}} - e^{-\frac{(z-2nd+z_0)^2}{4\gamma^2_{x,m}(t-t')}}\right)\right]. \quad (32)$$

The Green's function solutions for the infinite and semi-infinite geometries discussed until now have similar structure, inspiring us to attempt to write a generic expression for the remaining geometries considered in this work.

C. Generic Expression for Green's Function Solution

Equation (8) can be seen as a cascaded effect of three linear operators acting on $\Phi_m(\mathbf{r},t)$ for an impulse input $\delta(\mathbf{r}-\mathbf{r}',t-t')$, which results in the Green's function $g^{\text{fl}}_{\text{geo}}(\mathbf{r},\mathbf{r}',t,t')$ for a geometry.

Rewriting an operator equivalence of Eq. (8) as

$$L_\tau L_m L_x g^{\text{fl}}_{\text{geo}}(\mathbf{r},\mathbf{r}',t,t') = n\delta(\mathbf{r}-\mathbf{r}',t-t') \quad (33)$$

with

$$L_\tau = \left[1+\tau\frac{\partial}{\partial t}\right], \qquad L_m = \left[\gamma_m^2\nabla^2 - \mu_{am}c - \frac{\partial}{\partial t}\right], \qquad L_x = \left[\gamma_x^2\nabla^2 - \mu_{ax}c - \frac{\partial}{\partial t}\right]. \quad (34)$$

Irrespective of the rectangular Cartesian, cylindrical, or spherical polar coordinate systems in which the Laplacian operator is expressed, we generalize Eq. (25) and propose

$$g^{\phi_{\text{fl}}}_{\text{geo}}(\mathbf{r},\mathbf{r}',t,t') = \mathcal{C}[\gamma_x^2 g^{\phi_x}_{\text{geo}}(\mathbf{r},\mathbf{r}',t,t') - \gamma_m^2 g^{\phi_m}_{\text{geo}}(\mathbf{r},\mathbf{r}',t,t')] * \left[\frac{1}{\tau-\zeta^2}\left[\left(e^{-\frac{t}{\tau}} - e^{-\frac{t}{\zeta^2}}\right)u(t)\right]\right] \quad (35)$$

as the general form of the Green's function [3] for any geometry; i.e., $g^{\phi_{\text{fl}}}_{\text{geo}}(\mathbf{r},\mathbf{r}',t,t')$ as specified by Eq. (35) must satisfy Eq. (33), leading to finding an expression for $\mathcal{C}$. The proof is as shown below.

Substituting Eq. (35) into Eq. (33),

$$\mathcal{C}L_\tau\left(L_m\left(L_x\left([\gamma_x^2 g^{\phi_x}_{\text{geo}}(\mathbf{r},\mathbf{r}',t,t') - \gamma_m^2 g^{\phi_m}_{\text{geo}}(\mathbf{r},\mathbf{r}',t,t')] * \left[\frac{1}{\tau-\zeta^2}\left\{\left(e^{-\frac{t}{\tau}} - e^{-\frac{t}{\zeta^2}}\right)u(t)\right\}\right]\right)\right) = n\delta(\mathbf{r}-\mathbf{r}',t-t'). \quad (36)$$

Neglecting the constant $\mathcal{C}$ for now, the left-hand side (LHS) of the above equation can be written as

$$L_\tau\{\gamma_x^2 L_m(L_x(g^{\phi_x}_{\text{geo}}(\mathbf{r},\mathbf{r}',t,t'))) - \gamma_m^2 L_m(L_x(g^{\phi_m}_{\text{geo}}(\mathbf{r},\mathbf{r}',t,t')))\} * \left[\frac{1}{\tau-\zeta^2}\left\{\left(e^{-\frac{t}{\tau}} - e^{-\frac{t}{\zeta^2}}\right)u(t)\right\}\right]. \quad (37)$$

As the operators L_τ, L_m, L_x and convolution are linear operators, rewriting the second term of above expression leads to

$$L_\tau\{\gamma_x^2 L_m(L_x(g^{\phi_x}_{\text{geo}}(\mathbf{r},\mathbf{r}',t,t'))) - \gamma_m^2 L_x(L_m(g^{\phi_m}_{\text{geo}}(\mathbf{r},\mathbf{r}',t,t')))\} * \left[\frac{1}{\tau-\zeta^2}\left\{\left(e^{-\frac{t}{\tau}} - e^{-\frac{t}{\zeta^2}}\right)u(t)\right\}\right]. \quad (38)$$

As per the definition of the Green's function, we have

$$L_x(g^{\phi_x}_{\text{geo}}(\mathbf{r},\mathbf{r}',t,t')) = \delta(\mathbf{r}-\mathbf{r}',t-t'), \qquad L_m(g^{\phi_m}_{\text{geo}}(\mathbf{r},\mathbf{r}',t,t')) = \delta(\mathbf{r}-\mathbf{r}',t-t'). \quad (39)$$

Substituting Eq. (39) into Eq. (38) gives rise to

$$L_\tau\{\gamma_x^2 L_m(\delta(\mathbf{r}-\mathbf{r}',t-t')) - \gamma_m^2 L_x(\delta(\mathbf{r}-\mathbf{r}',t-t'))\} * \left[\frac{1}{\tau-\zeta^2}\left\{\left(e^{-\frac{t}{\tau}} - e^{-\frac{t}{\zeta^2}}\right)u(t)\right\}\right], \quad (40)$$

which can be equivalently written as

$$L_\tau\{\gamma_x^2 L_m - \gamma_m^2 L_x\}(\delta(\mathbf{r}-\mathbf{r}',t-t')) * \left[\frac{1}{\tau-\zeta^2}\left\{\left(e^{-\frac{t}{\tau}} - e^{-\frac{t}{\zeta^2}}\right)u(t)\right\}\right] \quad (41)$$

$$= L_\tau\left\{(\gamma_m^2\mu_{ax}c - \gamma_x^2\mu_{am}c) + (\gamma_m^2-\gamma_x^2)\frac{\partial}{\partial t}\right\}(\delta(\mathbf{r}-\mathbf{r}',t-t')) * \left[\frac{1}{\tau-\zeta^2}\left\{\left(e^{-\frac{t}{\tau}} - e^{-\frac{t}{\zeta^2}}\right)u(t)\right\}\right] \quad (42)$$

$$= \left(1+\tau\frac{\partial}{\partial t}\right)\left(A + B\frac{\partial}{\partial t}\right)(\delta(\mathbf{r}-\mathbf{r}',t-t')) * \left[\frac{1}{\tau-\zeta^2}\left\{\left(e^{-\frac{t}{\tau}} - e^{-\frac{t}{\zeta^2}}\right)u(t)\right\}\right]. \quad (43)$$

where $A = (\gamma_m^2\mu_{ax}c - \gamma_x^2\mu_{am}c)$, $B = (\gamma_m^2 - \gamma_x^2)$.

We may write $\delta(\mathbf{r}-\mathbf{r}',t-t') = \delta(\mathbf{r}-\mathbf{r}')\delta(t-t')$, and using the time shift property of the Dirac delta function, the LHS given by Eq. (43) can be simplified and substituted in Eq. (36) leading to

$$\mathcal{C}\frac{1}{\tau-\zeta^2}\left(1+\tau\frac{\partial}{\partial t}\right)\left(A+B\frac{\partial}{\partial t}\right)\left\{\left(e^{-\frac{t-t'}{\tau}}-e^{-\frac{t-t'}{\zeta^2}}\right)u(t-t')\right\} = n\delta(t-t'). \tag{44}$$

Once again, neglecting the constants for now, the LHS of the above equation can be written as

$$\left(A+(A\tau+B)\frac{\partial}{\partial t}+B\tau\frac{\partial^2}{\partial t^2}\right)\left\{\left(e^{-\frac{t-t'}{\tau}}-e^{-\frac{t-t'}{\zeta^2}}\right)u(t-t')\right\}. \tag{45}$$

As the above expression has an exponent in t and t', we consider the following two cases to show that the above expression is equivalent to the Dirac delta function ($\delta(t-t')$).

Case 1: $t > t'$

Writing an equivalent expression of Eq. (45),

$$A\left(e^{-\frac{t-t'}{\tau}}-e^{-\frac{t-t'}{\zeta^2}}\right)+(A\tau+B)\left(\frac{1}{\zeta^2}e^{-\frac{t-t'}{\zeta^2}}-\frac{1}{\tau}e^{-\frac{t-t'}{\tau}}\right)+B\tau\left(\frac{1}{\tau^2}e^{-\frac{t-t'}{\tau}}-\frac{1}{\zeta^4}e^{-\frac{t-t'}{\zeta^2}}\right). \tag{46}$$

Upon simplifying and collecting like terms together, we have

$$\left(1-\frac{\tau}{\zeta^2}\right)\left(\frac{B}{\zeta^2}-A\right)e^{-\frac{t-t'}{\zeta^2}}. \tag{47}$$

But by definition, $(B/\zeta^2)-A=0$, making Eq. (45) identically equal to zero $\forall\ t\neq t'$ (as $u(t-t')=0\ \forall\ t<t'$).

Case 2: $t=t'_+$

Using the chain rule of differentiation in the expression given by Eq. (45) leads to

$$\left\{\left(A+(A\tau+B)\frac{\partial}{\partial t}+B\tau\frac{\partial^2}{\partial t^2}\right)\left(e^{-\frac{t-t'}{\tau}}-e^{-\frac{t-t'}{\zeta^2}}\right)\right\}u(t-t') + \left(e^{-\frac{t-t'}{\tau}}-e^{-\frac{t-t'}{\zeta^2}}\right)\left\{\left(Au(t-t')+(A\tau+B)\delta(t-t')+B\tau\frac{\partial}{\partial t}\delta(t-t')\right)\right\}. \tag{48}$$

The first term is identically zero as per **Case 1**, leaving us with the second term, which is simplified as

$$\left(e^{-\frac{t-t'}{\tau}}-e^{-\frac{t-t'}{\zeta^2}}\right)\left\{\left(Au(t-t')+(A\tau+B)\delta(t-t')+B\tau\frac{\partial}{\partial t}\delta(t-t')\right)\right\} = A\left(e^{-\frac{t-t'}{\tau}}-e^{-\frac{t-t'}{\zeta^2}}\right)\Big|_{t=t'}+(A\tau+B)\left(e^{-\frac{t-t'}{\tau}}-e^{-\frac{t-t'}{\zeta^2}}\right)\delta(t-t')\Big|_{t=t'} + B\tau\frac{\partial}{\partial t}\delta(t-t')\left(e^{-\frac{t-t'}{\tau}}-e^{-\frac{t-t'}{\zeta^2}}\right)\Big|_{t=t'}. \tag{49}$$

The first two terms on the RHS are zero; using the property of distributional derivatives given by $\delta'\phi=-\delta\phi'$ for functions such as the Dirac delta will lead to

$$B\tau\frac{\partial}{\partial t}\delta(t-t')\left(e^{-\frac{t-t'}{\tau}}-e^{-\frac{t-t'}{\zeta^2}}\right)\Big|_{t=t'} = B\tau\delta(t-t')\left(\frac{1}{\zeta^2}e^{-\frac{t-t'}{\zeta^2}}-\frac{1}{\tau}e^{-\frac{t-t'}{\tau}}\right)\Big|_{t=t'} = \frac{B(\tau-\zeta^2)}{\zeta^2}\delta(t-t'). \tag{50}$$

Substituting in Eq. (44) and explicit writing of the terms leads to

$$\mathcal{C}\frac{1}{\tau-\zeta^2}\left(1+\tau\frac{\partial}{\partial t}\right)\left(A+B\frac{\partial}{\partial t}\right)\left\{\left(e^{-\frac{t-t'}{\tau}}-e^{-\frac{t-t'}{\zeta^2}}\right)u(t-t')\right\} = \mathcal{C}\frac{B}{\zeta^2}\delta(t-t')=n\delta(t-t'). \tag{51}$$

Comparing the coefficients, we have

$$\mathcal{C}\frac{B}{\zeta^2}=n \quad \text{or} \quad \mathcal{C}=\frac{n\zeta^2}{\gamma_m^2-\gamma_x^2}. \tag{52}$$

This leads to the conclusion that irrespective of the geometry under consideration the Green's function solution for the coupled differential equations given by Eqs. (1) and (2) can be expressed as

$$g_{\text{geo}}^{\phi_{\text{fl}}}(\mathbf{r},\mathbf{r}',t,t') = \frac{n\zeta^2}{\gamma_m^2-\gamma_x^2}[\gamma_x^2 g_{\text{geo}}^{\phi_x}(\mathbf{r},\mathbf{r}',t,t')-\gamma_m^2 g_{\text{geo}}^{\phi_m}(\mathbf{r},\mathbf{r}',t,t')] * \left[\frac{1}{\tau-\zeta^2}\left[\left(e^{-\frac{t}{\tau}}-e^{-\frac{t}{\zeta^2}}\right)u(t)\right]\right], \tag{53}$$

where $g_{\text{geo}}^{\phi_{x,m}}(\mathbf{r},\mathbf{r}',t,t')$ are the Green's function evaluated by substituting μ_{ax} and μ_{am}, respectively, in the diffusion equation with the Laplacian operator defined specifically to the relevant geometry under consideration.

The main derived quantity in the mathematical model for diffuse fluorescence spectroscopy/imaging is the photon flux, which can be calculated from the continuity equation (CE) for the photon density [from Eqs. (1) and (2)], where CE is defined as

$$\frac{\partial\Phi_{\text{fl}}}{\partial t}+\nabla\cdot\Gamma_{\text{fl}}(\xi,t)=-\mu_{am}c\Phi_{\text{fl}}, \tag{54}$$

where $\Gamma_{\text{fl}}(\xi,t)$ is the photon flux. This, combined with the diffusion equation and the fact that Φ_{fl} can be written as the difference between the photon densities Φ_x, Φ_m by Eq. (53), leads to the following expression for the photon flux:

$$\Gamma_{\text{fl}}(\xi,t)=-\gamma_m^2\nabla\cdot\Phi_m(\mathbf{r},t)+\gamma_x^2\nabla\cdot\Phi_x(\mathbf{r},t), \tag{55}$$

where $\Phi_{\text{fl}}(\mathbf{r},t)$ is the diffuse photon density corresponding to $g_{\text{geo}}^{\phi_{\text{fl}}}(\mathbf{r},\mathbf{r}',t,t')$. We have a difference between the two fluxes in Eq. (53); by the above definition one can rewrite it as

$$\therefore g_{\text{geo}}^{\Gamma_{\text{fl}}}(\mathbf{r},\mathbf{r}',t,t') = \frac{n\zeta^2\gamma_m^2}{\gamma_m^2-\gamma_x^2}[g_{\text{geo}}^{\Gamma_x}(\mathbf{r},\mathbf{r}',t,t')-g_{\text{geo}}^{\Gamma_m}(\mathbf{r},\mathbf{r}',t,t')] * \left[\frac{1}{\tau-\zeta^2}\left[\left(e^{-\frac{t}{\tau}}-e^{-\frac{t}{\zeta^2}}\right)u(t)\right]\right], \tag{56}$$

where $g_{\text{geo}}^{\Gamma_x}(\mathbf{r},\mathbf{r}',t,t')=-\gamma_x^2\nabla\cdot g_{\text{geo}}^{\phi_x}(\mathbf{r},\mathbf{r}',t,t')$ and $g_{\text{geo}}^{\Gamma_m}(\mathbf{r},\mathbf{r}',t,t')=-\gamma_m^2\nabla\cdot g_{\text{geo}}^{\phi_m}(\mathbf{r},\mathbf{r}',t,t')$.

For the frequency-domain case, the expression becomes (Fourier transform of the above equation)

Table 2. Green's Function Solution in the Time-Domain Case for Planar Type Geometries, where $p = x$ or m

Geometry	$g_{\text{geo}}^{\Gamma_p}$ (*Time Domain*)	
Infinite	$\frac{d}{2\sqrt{(4\pi\gamma_p^2)^3(t-t')^5}} e^{-\left(\mu_{ap}c(t-t')+\frac{d^2}{4\gamma_p^2(t-t')}\right)}$	(g01)
Semi-infinite half-space	$\frac{1}{2\sqrt{(4\pi\gamma_p^2)^3(t-t')^5}}\left[d_1 e^{-\left(\mu_{ap}c(t-t')+\frac{\rho_1^2}{4\gamma_p^2(t-t')}\right)} + d_2 e^{-\left(\mu_{ap}c(t-t')+\frac{\rho_2^2}{4\gamma_p^2(t-t')}\right)}\right]$	(g02)
ZBC	$d_1 = d_2 = z_0,\ \rho_1 = \rho_2 = \rho$	
EBC	$d_1 = z_0,\ d_2 = (z_0 + 2z_e),\ \rho_1 = \rho,\ \rho_2 = \grave{\rho}$	
Infinite slab (at $z = d$)	$-\frac{e^{-\mu_{ap}c(t-t')}}{\sqrt{(4\pi\gamma_p^2)^3(t-t')^5}}\sum_{n=0}^{\infty}\left[d_1 e^{-\frac{\rho_1^2}{4\gamma_p^2(tc-t')}} - d_2 e^{-\frac{\rho_2^2}{4\gamma_p^2(tc-t')}}\right]$	(g03)
ZBC	$d_1 = z_{+n},\ d_2 = z_{-n},\ \rho_1 = \rho_{+n},\ \rho_2 = \rho_{-n}$	
EBC	$d_1 = \grave{z}_{+n},\ d_2 = \grave{z}_{-n},\ \rho_1 = \grave{\rho}_{+n},\ \rho_2 = \grave{\rho}_{-n}$	
Infinite slab (at $z = 0$)	$\frac{e^{-\mu_{ap}c(t-t')}}{\sqrt{(4\pi\gamma_p^2)^3(t-t')^5}}\left\{z_0 e^{-\frac{\rho^2}{4\gamma_p^2(tc-t')}} + \sum_{n=1}^{\infty}\left[d_1 e^{-\frac{\rho_1^2}{4\gamma_p^2(tc-t')}} - d_2 e^{-\frac{\rho_2^2}{4\gamma_p^2(tc-t')}}\right]\right\}$	(g04)
ZBC	$d_1 = z_{+n'},\ d_2 = z_{-n'},\ \rho_1 = \rho_{+n'},\ \rho_2 = \rho_{-n'}$	
EBC	$d_1 = \grave{z}_{+n'},\ d_2 = \grave{z}_{-n'},\ \rho_1 = \grave{\rho}_{+n'},\ \rho_2 = \grave{\rho}_{-n'}$	

$$\therefore G_{\text{geo}}^{\Gamma_{\mathbb{n}}}(\mathbf{r},\mathbf{r}',\omega,t') = \frac{n\zeta^2}{\gamma_m^2-\gamma_x^2}[G_{\text{geo}}^{\Gamma_x}(\mathbf{r},\mathbf{r}',\omega,t') - G_{\text{geo}}^{\Gamma_m}(\mathbf{r},\mathbf{r}',\omega,t')] \cdot\left[\frac{1}{\tau-\zeta^2}\left\{\frac{1}{\frac{1}{\tau}+j\omega}-\frac{1}{\frac{1}{\zeta^2}+j\omega}\right\}\right]. \quad (57)$$

Note that similar to the diffusion equation solutions as given in [5], we have also listed the expressions for $g_{\text{geo}}^{\Gamma_{\mathbb{n}}}(\mathbf{r},\mathbf{r}',t,t')$ and $G_{\text{geo}}^{\Gamma_{\mathbb{n}}}(\mathbf{r},\mathbf{r}',\omega,t')$ in case of various geometries in Tables 2 and 3 and Tables 4 and 5, respectively, for this case of ZBC. These expressions are derived from the Green's function solution for the heat equation as given in [12]. Note that the data types, which are typically measured in a typical experiment, will use these forms to arrive at closed-form expressions, and the same is given in Section 5.

4. EXTRAPOLATED BOUNDARY CONDITION

A useful simplifying assumption for solving the coupled diffusion equations is that all the incident photons are initially scattered isotropically at a depth $z_0 = 1/\mu'_{sx}$ below the surface. The geometry for calculation of the time-resolved transmittance for a homogeneous slab for the ZBC or Dirichlet boundary condition is shown in Fig. 2. The average diffuse intensity is set to zero at the surface of the slab at $z = 0$. As stated above, the source is assumed to be located a distance z_0 into the medium. Thus a negative image source must be located at the distance $z = -z_0$ to meet the boundary condition. The boundary condition for the surface located at $z = d$ is satisfied by the dipole centered about $z = 2d$, but then the boundary condition at $z = 0$ is violated. Both boundary conditions can only be met simultaneously by adding an infinite number of dipoles. In practice, the number of dipoles required depends on the background optical properties of the slab and the maximum time for which the transmittance is calculated.

However, ZBC is not sufficient when there is a mismatch between the refractive index of the diffusing and the surrounding medium resulting in ZBC on an extrapolated boundary at a distance $z_e = 2\mathbb{A}\mu'_{sx}$ from the true boundary [6]. Here defining n as the ratio of refractive indices between the free space (air) and tissue and representing μ'_{sx} as the reduced scattering coefficient [6] defines $\mathbb{A}$ as

$$\mathbb{A} = \frac{1+\frac{3}{2}\left[\frac{8(1-n^2)^{3/2}}{105n^3} - \frac{(n-1)^2(8+32n+52n^2+13n^3)}{105n^3(1+n)^2} + r_1(n) + r_2(n) + r_3(n)\right]}{1-\frac{-3+7n+13n^2+9n^3-7n^4+3n^5+n^6+n^7}{3(n-1)(n+1)^2(n^2+1)^2} - r_4(n)},$$

$$r_1(n) = \frac{-4+n-4n^2+25n^3-40n^4-6n^5+8n^6+30n^7-12n^8+n^9+n^{11}}{3n(n^2-1)^2(n^2+1)^3},$$

$$r_2(n) = \frac{2n^3(3+2n^4)}{(n^2-1)^2(n^2+1)^{7/2}}\log\left\{\frac{n^2[n-(1+n^2)^{1/2}][2+n^2+2(1+n^2)^{1/2}]}{[n+(1+n^2)^{1/2}][-2+n^4-2(1-n^4)^{1/2}]}\right\}, \quad (58)$$

Table 3. Green's Function Solution in the Time-Domain Case for Circular Type Geometries, where $p = x$ or m

Geometry	$g_{\text{geo}}^{\Gamma_p}$ (*Time Domain*)	
2D circle, radius a	$\frac{\gamma_p^2 e^{-\mu_{ap}c(t-t')}}{\pi q^2}\sum_{n=-\infty}^{\infty}\left[\cos(n\theta)\sum_{\beta_n} e^{-\gamma_p^2\beta_n^2(t-t')}\beta_n f_n(\beta_n r', \beta_n q)\right]$	(g05)
Finite cylinder, radius a, length l	$\frac{2\gamma_p^2 e^{-\mu_{ap}c(t-t')}}{\pi q^2 l}\sum_{k=1,\text{odd}}^{\infty} e^{-\frac{\gamma_p^2 k^2\pi^2(t_{\kappa}-t')}{l^2}}\sum_{n=-\infty}^{\infty}\left[\cos(n\theta)\sum_{\beta_n} e^{-\gamma_p^2\beta_n^2(t-t')}\beta_n f_n(\beta_n r', \beta_n q)\right]$	(g06)
Infinite cylinder, radius a, $z = z'$	$\frac{\gamma_p e^{-\mu_{ap}c(t-t')}}{2\pi q^2\sqrt{\pi(t-t')}}\sum_{n=-\infty}^{\infty}\cos(n\theta)\sum_{\beta_n} e^{-\gamma_p^2\beta_n^2(t-t')}\beta_n f_n(\beta_n r', \beta_n q)$	(g07)
Sphere, radius a	$\frac{\gamma_p^2 e^{-\mu_{ap}c(t-t')}}{2\pi q^2\sqrt{ar'}}\sum_{n=0}^{\infty}\sum_{\beta_{n+\frac{1}{2}}} e^{-\gamma_p^2\beta_{n+\frac{1}{2}}^2(t-t')}\beta_{n+\frac{1}{2}} f_{n+\frac{1}{2}}(\beta_{n+\frac{1}{2}}r', \beta_{n+\frac{1}{2}}q)(2n+1)P_n(\cos\theta)$	(g08)
Note:	For all the circular geometries, such as the 2D circle, cylinder, and sphere, we have	
ZBC	$q = a, f_n(\beta_n r', \beta_n q) = \frac{J_n(\beta_n r')}{J_{n+1}(\beta_n q)}$	
EBC	$q = b, f_n(\beta_n r', \beta_n q) = \frac{J_n'(\beta_n a)J_n(\beta_n r')}{(J_{n+1}(\beta_n q))^2}$	

Table 4. Green's Function Solution in the Frequency-Domain Case for Planar Type Geometries, where $p = x$ or m

Geometry	$G_{\text{geo}}^{\Gamma_p}$ (*Frequency Domain*)	
Infinite	$e^{-j\omega t'}(1+\alpha_p d)\frac{e^{-\alpha_p d}}{2\sqrt{(2\pi)^3 d^2}}$	(G01)
Semi-infinite half-space	$\frac{e^{-j\omega t'}}{2(2\pi)^{3/2}}\left[(1+\alpha_p\rho_1)\frac{d_1 e^{-\alpha_p\rho_1}}{\rho_1^3}+(1+\alpha_p\rho_2)\frac{d_2 e^{-\alpha_p\rho_2}}{\rho_2^3}\right]$	(G02)
ZBC	$d_1 = d_2 = z_0,\ \rho_1 = \rho_2 = \rho$	
EBC	$d_1 = z_0,\ d_2 = (z_0 + 2z_e),\ \rho_1 = \rho,\ \rho_2 = \grave{\rho}$	
Infinite slab (at $z = d$)	$-\frac{e^{-j\omega t'}}{\sqrt{(2\pi)^3}}\left(\sum_{n=0}^{\infty}\left[(1+\alpha_p\rho_1)\frac{d_1}{\rho_1^3}e^{-\alpha_p\rho_1}-(1+\alpha_p\rho_2)\frac{d_2}{\rho_2^3}e^{-\alpha_p\rho_2}\right]\right)$	(G03)
ZBC	$d_1 = z_{+n},\ d_2 = z_{-n},\ \rho_1 = \rho_{+n},\ \rho_2 = \rho_{-n}$	
EBC	$d_1 = \grave{z}_{+n},\ d_2 = \grave{z}_{-n},\ \rho_1 = \grave{\rho}_{+n},\ \rho_2 = \grave{\rho}_{-n}$	
Infinite slab (at $z = 0$)	$\frac{e^{-j\omega t'}}{\sqrt{(2\pi)^3}}\left((1+\alpha_p\rho)\frac{z_0}{\rho^3}e^{-\alpha_p\rho}+\sum_{n=1}^{\infty}\left[(1+\alpha_p\rho_1)\frac{d_1}{\rho_1^3}e^{-\alpha_p\rho_1}-(1+\alpha_p\rho_2)\frac{d_2}{\rho_2^3}e^{-\alpha_p\rho_2}\right]\right)$	(G04)
ZBC	$d_1 = z_{+n'},\ d_2 = z_{-n'},\ \rho_1 = \rho_{+n'},\ \rho_2 = \rho_{-n'}$	
EBC	$d_1 = \grave{z}_{+n'},\ d_2 = \grave{z}_{-n'},\ \rho_1 = \grave{\rho}_{+n'},\ \rho_2 = \grave{\rho}_{-n'}$	

$$r_3(n) = \frac{4(1-n^2)^{1/2}(1+12n^4+2n^8)}{3n(n^2-1)^2(n^2+1)^3},$$
$$r_4(n) = \frac{(1+6n^4+n^8)\log\left(\frac{1-n}{1+n}\right)+4(n^2+n^6)\log\left[\frac{1+n}{n^2(1-n)}\right]}{(n^2-1)^2(n^2+1)^3}. \quad (59)$$

Note that typical tissue refractive index is considered to be 1.33, and the free space is considered to be 1, resulting in $n < 1$.

The extrapolated boundaries for infinite slab and circular geometries are depicted in Figs. 3 and 4, respectively. In the following derivations we would determine the Green's function for the equation

Time-domain case:

$$\left[\gamma^2\nabla^2 - \mu_a c - \frac{\partial}{\partial t}\right]\Phi(\mathbf{r}, t) = -q_0(\mathbf{r}, t). \quad (60)$$

Frequency-domain case:

$$-[k^2\gamma^2 + \mu_a c + j\omega]\Phi(\mathbf{k}, \omega) = -Q_0(\mathbf{k}, \omega). \quad (61)$$

by using suitable suffixes to the Green's function solutions of the above equations combining with the result of

Table 5. Green's Function Solution in the Frequency-Domain Case for Circular Type Geometries, where $p = x$ or m

Geometry	$G^{\Gamma_p}_{\text{geo}}$ (*Frequency Domain*)	
2D circle, radius a	$\frac{e^{-j\omega t'}}{\sqrt{(2\pi)^3}} \sum_{n=-\infty}^{\infty} \cos(n\theta) f_n(\alpha_p r')$	(G05)
Finite cylinder, radius a, length l	$\frac{e^{-j\omega t'}}{\pi\sqrt{2\pi l}} \sum_{k=1,\text{odd}}^{\infty} \sum_{n=-\infty}^{\infty} \cos(n\theta) f_n(\alpha_{pk} r')$	(G06)
Infinite cylinder, radius a, $z = z'$	$\frac{e^{-j\omega t'}}{\sqrt{(2\pi)^3}} \sum_{n=-\infty}^{\infty} \cos(n\theta) \sum_{\beta_n} \frac{1}{\sqrt{\alpha_p^2 + \beta_n^2}} \beta_n g_n(\beta_n r')$	(G07)
Sphere, radius a	$\frac{e^{-j\omega t'}}{2\sqrt{(2\pi)^3 q r'}} \sum_{n=0}^{\infty} (2n+1) P_n(\cos\theta) f_{n+1/2}(r'\alpha_p)$	(G08)
Note:	For all the circular geometries, such as the 2D circle, cylinder, and sphere, we have	
ZBC	$q = a, f_n(\varepsilon r') = \frac{1}{a}\frac{I_n(r'\varepsilon)}{I_n(a\varepsilon)}$, $g_n(\varepsilon r') = \frac{1}{a^2}\frac{J_n(r'\varepsilon)}{J_{n+1}(a\varepsilon)}$	
EBC	$q = b, f_n(\varepsilon r') = \frac{\varepsilon I_n(r'\varepsilon)}{I_n(b\varepsilon)} F'_n(a\varepsilon, b\varepsilon)$, $g_n(\varepsilon r') = \frac{1}{b^2}\frac{J'_n(a\varepsilon)J_n(r'\varepsilon)}{(J_{n+1}(b\varepsilon))^2}$	
	$F'_n(a\varepsilon, b\varepsilon) = \frac{-n}{a\varepsilon} F_n(a\varepsilon, b\varepsilon) - (I_{n-1}(a\varepsilon)K_n(b\varepsilon) + K_{n-1}(a\varepsilon)I_n(b\varepsilon))$	
	$F_n(a\varepsilon, b\varepsilon) = K_n(a\varepsilon)I_n(b\varepsilon) - I_n(a\varepsilon)K_n(b\varepsilon)$	

Eq. (53) using the EBC for arriving at a more generic form. The Green's functions for the EBC, which is a more realistic condition compared to ZBC, in the time domain and the frequency domain are given by $\grave{g}^{\phi}_{\text{geo}}(\mathbf{r}, \mathbf{r}', t, t')$ and $\grave{G}^{\phi}_{\text{geo}}(\mathbf{r}, \mathbf{r}', \omega, t')$, respectively, for each relevant geometry dropping suffixes x, m.

Figure 3 shows the dipole arrangement necessary to achieve zero flux on the extrapolated boundary. Initially, we derive the expression for $\grave{g}^{\phi}_{\text{geo}}(\mathbf{r}, \mathbf{r}', t, t')$ and $\grave{G}^{\phi}_{\text{geo}}(\mathbf{r}, \mathbf{r}', \omega, t')$ in planar geometries such as semi-infinite and infinite slabs when subjected to EBC. Note that the infinite geometry solution is not affected by the boundary condition, as the boundary does not exist. So for infinite geometry, the Green's function solutions are the same for both ZBC and EBC (Section 3.A gives these expressions).

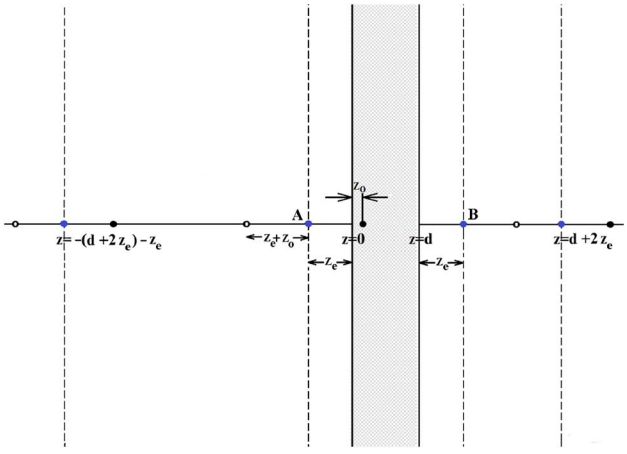

Fig. 3. (Color online) Illustration of the extrapolated boundary for infinite slab geometry with source dipoles. The actual domain is the shaded region.

A. Case 1: Semi-Infinite Geometry

Figure 2 shows the ZBC for the semi-infinite geometry; now assume an extrapolated boundary exists at a distance $-z_e$. In order to satisfy the ZBC on the extended boundary, Eq. (30) needs to be modified as

$$\grave{g}^{\phi}_{\text{half}}(\mathbf{r}, \mathbf{r}', t, t') = \frac{e^{-\left[\mu_a c(t-t') + \frac{\xi^2}{4\gamma^2(t-t')}\right]}}{[4\pi\gamma^2(t-t')]^{3/2}} \left[e^{-\frac{(z-z_0)^2}{4\gamma^2(t-t')}} - e^{-\frac{(z+z_0+2z_e)^2}{4\gamma^2(t-t')}} \right]. \tag{62}$$

Taking the Fourier transform we have

$$\grave{G}^{\phi}_{\text{half}}(\mathbf{r}, \mathbf{r}', \omega, t') = \frac{e^{-j\omega t'}}{2(2\pi)^{3/2}\gamma^2} \left\{ \frac{e^{-\alpha(\xi^2 + (z-z_0)^2)^{1/2}}}{[\xi^2 + (z-z_0)^2]^{1/2}} - \frac{e^{-\alpha(\xi^2 + (z+z_0+2z_e)^2)^{1/2}}}{[\xi^2 + (z+z_0+2z_e)^2]^{1/2}} \right\}. \tag{63}$$

B. Case 2: Infinite Slab Geometry

Figure 3 shows the extended boundary for the infinite slab geometry. In order to satisfy the ZBC on the extended boundary, Eq. (31) needs to be modified as

$$\grave{g}^{\phi}_{\text{slab}}(\mathbf{r}, \mathbf{r}', t, t') = \frac{e^{-\left[\mu_a c(t-t') + \frac{\xi^2}{4\gamma^2(t-t')}\right]}}{[4\pi\gamma^2(t-t')]^{3/2}} \left[\sum_{n=-\infty}^{\infty} \left\{ e^{-\frac{(z-\hat{z}+n)^2}{4\gamma^2(t-t')}} - e^{-\frac{(z-\hat{z}-n)^2}{4\gamma^2(t-t')}} \right\} \right]. \tag{64}$$

Taking the Fourier transform we have the Green's function in the frequency domain

$$\grave{G}^{\phi}_{\text{slab}}(\mathbf{r},\mathbf{r}',\omega,t') = \frac{e^{-j\omega t'}}{2(2\pi)^{3/2}}\left[\sum_{n=-\infty}^{\infty}\left\{\frac{e^{-\alpha(\xi^2+(z-\grave{z}_{+n})^2)^{1/2}}}{[\xi^2+(z-\grave{z}_{+n})^2]^{1/2}} - \frac{e^{-\alpha(\xi^2+(z-\grave{z}_{-n})^2)^{1/2}}}{[\xi^2+(z-\grave{z}_{-n})^2]^{1/2}}\right\}\right]. \quad (65)$$

C. Case 3: Circle

Figure 4 shows the source-detector placement in a circular geometry with the extrapolated boundary. In this section, we derive the expression for $g^{\Gamma_{\text{fl}}}_{\text{geo}}(\mathbf{r},\mathbf{r}',t,t')$ and $G^{\Gamma_{\text{fl}}}_{\text{geo}}(\mathbf{r},\mathbf{r}',\omega,t')$ for the circle initially and extend it to other circular geometries, such as a cylinder and a sphere when subjected to EBC.

We consider the circle as a cross section along a plane perpendicular to the axis of an infinite cylinder with an infinite source along its axis. We will derive this form in detail, as it will act as a precursor to determine the analytical solution for other circular domains. Starting with the two-dimensional form of the Green's function for an infinite medium [5] as the plausible solution for the circular geometry,

$$g^{\phi}_{\text{cir}}(\mathbf{r},\mathbf{r}',t,t') = \frac{1}{4\pi\gamma^2(t-t')}e^{-\left(\mu_a c(t-t')+\frac{|\mathbf{r}-\mathbf{r}'|^2}{4\gamma^2(t-t')}\right)},$$

$$G^{\phi}_{\text{cir}}(\mathbf{r},\mathbf{r}',\omega,t') = \frac{e^{-j\omega t'}}{(2\pi)^{3/2}\gamma^2}K_0(\alpha|\mathbf{r}-\mathbf{r}'|).$$

The auxiliary equation for circular geometry in the Fourier domain is

$$\left(\frac{\partial^2}{\partial\mathbf{r}^2}+\frac{1}{\mathbf{r}}\frac{\partial}{\partial\mathbf{r}}+\frac{1}{\mathbf{r}^2}\frac{\partial^2}{\partial\theta^2}-\alpha^2\right)H^{\phi}(\mathbf{r},\omega)=0, \quad (66)$$

which has a general solution of the form $H^{\phi}(\mathbf{r},\omega) = \sum_{n=-\infty}^{\infty}[a_nI_n(r\alpha)+b_nK_n(r\alpha)]\cos(n\theta)$, where I_n and K_n are modified Bessel functions of the first and second kind of order n, respectively.

We make use of the addition theorem for the Bessel function $K_0(\alpha|\mathbf{r}-\mathbf{r}'|)$ as given in Section 11.4 in [13],

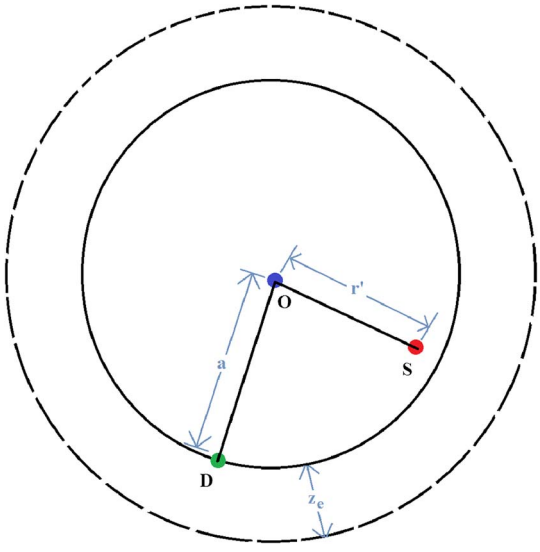

Fig. 4. (Color online) Illustration of the extrapolated boundary (dashed line) for circular geometry; the solid line shows the actual boundary.

$$K_0(\alpha|\mathbf{r}-\mathbf{r}'|) = \begin{cases}\sum_{n=-\infty}^{\infty}\cos(n\theta)I_n(r'\alpha)+b_nK_n(r\alpha), & r>r'\\ \sum_{n=-\infty}^{\infty}\cos(n\theta)I_n(r\alpha)+b_nK_n(r'\alpha), & r<r'\end{cases}, \quad (67)$$

and find a_n, b_n such that $G^{\phi}_{\text{cir}}+H^{\phi}=0$ on the extrapolated boundary $r=b$. This leads to $b_n=0$ and $a_n = -(K_n(b\alpha)I_n(r'\alpha))/I_n(b\alpha)$ resulting in

$$\grave{G}^{\phi}_{\text{cir}}(\mathbf{r},\mathbf{r}',\omega,t') = \frac{e^{-j\omega t'}}{(2\pi)^{3/2}\gamma^2}\sum_{n=-\infty}^{\infty}\left[\cos(n\theta)\frac{I_n(r'\alpha)}{I_n(b\alpha)}F_n(r\alpha,b\alpha)\right], \quad (68)$$

where $F_n(r\alpha,b\alpha) = K_n(r\alpha)I_n(b\alpha) - I_n(r\alpha)K_n(b\alpha)$ for $r>r'$. In the case of $r<r'$, we interchange r and r' in the above expression. Taking the inverse Fourier transform results in the time-domain form as

$$\grave{g}^{\phi}_{\text{cir}}(\mathbf{r},\mathbf{r}',t,t') = \frac{1}{2\pi}\sum_{n=-\infty}^{\infty}\left[\cos(n\theta)\times\int_0^{\infty}e^{j\omega(t-t')}\frac{I_n(r'\alpha)}{I_n(b\alpha)}F_n(r\alpha,b\alpha)\mathrm{d}\omega\right]. \quad (69)$$

This can be evaluated by considering a closed contour consisting of the real axis and a large semicircle in the upper half-plane for $t>t'$. This contour cannot pass through any poles on the imaginary axis at the zeros of $J_n(b\alpha)$. This can be realized by using the identity $I_n(ze^{\pm j(\pi/2)}) = e^{\pm j(n\pi/2)}J_n(z)$, where J_n is the Bessel function of order n, and the fact that the equation $J_n(z)=0$ has an infinite number of distinct real roots [14]. Evaluating the residues over all these poles gives the final expression as

$$\grave{g}^{\phi}_{\text{cir}}(\mathbf{r},\mathbf{r}',t,t') = \frac{e^{-\mu_a c(t-t')}}{2\pi a}\sum_{n=-\infty}^{\infty}\left[\cos(n\theta)\times\sum_{\beta_n}e^{-\gamma^2\beta_n^2(t-t')}\frac{J_n(\beta_n r)J_n(\beta_n r')}{(J'_n(\beta_n b))^2}\right]. \quad (70)$$

D. Case 4: Finite Cylinder

In this case the auxiliary equation in the Fourier domain becomes

$$\left(\frac{1}{\mathbf{r}^2}\frac{\partial^2}{\partial\theta^2}+\frac{\partial^2}{\partial\mathbf{r}^2}+\frac{1}{\mathbf{r}}\frac{\partial}{\partial\mathbf{r}}+\frac{\partial^2}{\partial\mathbf{z}^2}-\alpha^2\right)H^{\phi}(\mathbf{r},\omega)=0, \quad (71)$$

which has a general solution of the form

$$H^{\phi}(\mathbf{r},\omega) = \sum_{m,n}^{\infty}[\![a_{m,n}I_n\left(r\left[\alpha^2+\left(\frac{m\pi}{l}\right)^2\right]^{1/2}\right) + b_{m,n}K_n\left(r\left[\alpha^2+\left(\frac{m\pi}{l}\right)^2\right]^{1/2}\right)]\!] \times\cos(n\theta)\sin\left(\frac{m\pi z}{l}\right).$$

We make use of the addition theorem for the Bessel function $K_0(\alpha|\mathbf{r}-\mathbf{r}'|)$ similar to the above case leading to $b_{m,n}=0$ and

$$a_{m,n} = -\frac{I_n\left(r'\left[\alpha^2 + \left(\frac{m\pi}{l}\right)^2\right]^{1/2}\right)K_n\left(b\left[\alpha^2 + \left(\frac{m\pi}{l}\right)^2\right]^{1/2}\right)}{I_n\left(r'\left[\alpha^2 + \left(\frac{m\pi}{l}\right)^2\right]^{1/2}\right)}$$

with m being an *odd number* or otherwise 0. We proceed as in the previous case and arrive at the following expressions for the Green's functions in time and frequency domains, respectively:

$$\grave{g}^{\phi}_{\mathrm{fcyl}}(\mathbf{r},\mathbf{r}',z,z',t,t') = \frac{e^{-\left(\mu_a c(t-t') + \frac{(z-z')^2}{4\gamma^2(t-t')}\right)}}{\pi a l}\sum_{m=1,\mathrm{odd}}^{\infty} e^{-\gamma^2\frac{m^2\pi^2}{l^2}(t-t')} \times \sum_{n=-\infty}^{\infty}\left[\cos(n\theta)\sum_{\beta_n} e^{-\gamma^2\beta_n^2(t-t')}\frac{J_n(\beta_n r)J_n(\beta_n r')}{(J_n'(\beta_n b))^2}\right], \quad (72)$$

$$\grave{G}^{\phi}_{\mathrm{fcyl}}(\mathbf{r},\mathbf{r}',\omega,t')|_{z=z'} = \frac{e^{-j\omega t'}}{(2\pi)^{3/2}l}\sum_{m=1,\mathrm{odd}}^{\infty}\sum_{n=-\infty}^{\infty} \times\left[\cos(n\theta)\frac{I_n(\alpha_m r')}{I_n(\alpha_m b)}F_n(\alpha_m r,\alpha_m b)\right]. \quad (73)$$

E. Case 5: Infinite Cylinder

The limiting case of the finite cylinder with the limit $l \to \infty$ will yield expressions for the infinite cylinder case; we consider

$$\grave{G}^{\phi}_{\mathrm{cyl}}(\mathbf{r},\mathbf{r}',z,\omega,t') = \frac{e^{-j\omega t'}}{(2\pi)^{3/2}b}\sum_{n=-\infty}^{\infty}\cos(n\theta) \times\int_0^{\infty}\frac{I_n\left(r'\sqrt{\alpha^2+z^2}\right)}{I_n\left(b\sqrt{\alpha^2+z^2}\right)} \times F_n\left(r\sqrt{\alpha^2+z^2}, b\sqrt{\alpha^2+z^2}\right)\mathrm{d}z. \quad (74)$$

Taking the inverse Fourier transform leads to (time-domain case)

$$\grave{g}^{\phi}_{\mathrm{cyl}}(\mathbf{r},\mathbf{r}',z,z',t,t') = \frac{e^{-\left(\mu_a c(t-t') + \frac{(z-z')^2}{4\gamma^2(t-t')}\right)}}{2\pi b^2\gamma\sqrt{\pi(t-t')}}\sum_{n=-\infty}^{\infty}\cos(n\theta) \times\sum_{\beta_n} e^{-\gamma^2\beta_n^2(t-t')}\frac{J_n(\beta_n r)J_n(\beta_n r')}{(J_n'(\beta_n b))^2}. \quad (75)$$

F. Case 6: Sphere

The auxiliary equation for a spherical geometry in the Fourier domain is defined as

$$\left(\frac{\partial^2}{\partial\mathbf{r}^2} + \frac{2\partial}{\mathbf{r}\partial\mathbf{r}} + \frac{1}{\mathbf{r}^2}\frac{1}{\sin\theta}\frac{\partial}{\partial\theta}\sin\theta\frac{\partial}{\partial\theta} - \alpha^2\right)H^{\phi}(\mathbf{r},\omega) = 0. \quad (76)$$

Considering solutions that are finite at the origin, the general solution to the auxiliary equation will be $H^{\phi}(\mathbf{r},\omega) = \sqrt{\pi/2\alpha r}\sum_n^{\infty} a_n I_{n+(1/2)}(r\alpha)P_n(\cos\theta)$, where P_n is Legendre polynomial of order n.

Table 6. Closed-form Expressions for Planar Type Geometries for Integrated Intensity $E^{\mathrm{fl}}_{\mathrm{geo}}(\xi) = (n\zeta^2\gamma_m^2/(\gamma_m^2 - \gamma_x^2))W^{\mathrm{fl}}_{\mathrm{geo}}(\xi)$

Geometry	$W^{\mathrm{fl}}_{\mathrm{geo}}(\xi)$	
Infinite	$\frac{(1+\sigma_x d)e^{-\sigma_x d} - (1+\sigma_m d)e^{-\sigma_m d}}{4\pi d^2}$	(I01)
Semi-infinite half-space	$\frac{1}{4\pi}\left[\frac{d_1((1+\sigma_x\rho_1)e^{-\sigma_x\rho_1} - (1+\sigma_m\rho_1)e^{-\sigma_m\rho_1})}{\rho_1^3} + \frac{d_2((1+\sigma_x\rho_2)e^{-\sigma_x\rho_2} - (1+\sigma_m\rho_2)e^{-\sigma_m\rho_2})}{\rho_2^3}\right]$	(I02)
ZBC	$d_1 = d_2 = z_0,\ \rho_1 = \rho_2 = \rho$	
EBC	$d_1 = z_0,\ d_2 = (z_0 + 2z_e),\ \rho_1 = \rho,\ \rho_2 = \grave{\rho}$	
Infinite slab $0 < z < d$ (at $z = d$)	$-\frac{1}{2\pi}\left[\sum_{n=0}^{\infty}\left\{\frac{d_1((1+\sigma_x\rho_1)e^{-\sigma_x\rho_1} - (1+\sigma_m\rho_1)e^{-\sigma_m\rho_1})}{\rho_1^3}\right\} - \sum_{n=0}^{\infty}\left\{\frac{d_2((1+\sigma_x\rho_2)e^{-\sigma_x\rho_2} - (1+\sigma_m\rho_2)e^{-\sigma_m\rho_2})}{\rho_2^3}\right\}\right]$	(I03)
ZBC	$d_1 = z_{+n},\ d_2 = z_{-n},\ \rho_1 = \rho_{+n},\ \rho_2 = \rho_{-n}$	
EBC	$d_1 = \grave{z}_{+n},\ d_2 = \grave{z}_{-n},\ \rho_1 = \grave{\rho}_{+n},\ \rho_2 = \grave{\rho}_{-n}$	
Infinite slab (at $z = 0$)	$\frac{1}{2\pi}\frac{z_0((1+\sigma_x\rho)e^{-\sigma_x\rho} - (1+\sigma_m\rho)e^{-\sigma_m\rho})}{\rho^3} + \frac{1}{2\pi}\sum_{n=1}^{\infty}\left(\frac{d_1((1+\sigma_x\rho_1)e^{-\sigma_x\rho_1} - (1+\sigma_m\rho_1)e^{-\sigma_m\rho_1})}{\rho_1^3}\right) - \frac{1}{2\pi}\sum_{n=1}^{\infty}\left(\frac{d_2((1+\sigma_x\rho_2)e^{-\sigma_x\rho_2} - (1+\sigma_m\rho_2)e^{-\sigma_m\rho_2})}{\rho_2^3}\right)$	(I04)
ZBC	$d_1 = z_{+n'},\ d_2 = z_{-n'},\ \rho_1 = \rho_{+n'},\ \rho_2 = \rho_{-n'}$	
EBC	$d_1 = \grave{z}_{+n'},\ d_2 = \grave{z}_{-n'},\ \rho_1 = \grave{\rho}_{+n'},\ \rho_2 = \grave{\rho}_{-n'}$	

Table 7. Closed-form Expressions for Circular Type Geometries for Integrated Intensity $E^{\mathrm{fl}}_{\mathrm{geo}}(\xi) = (n\zeta^2\gamma_m^2/(\gamma_m^2 - \gamma_x^2))W^{\mathrm{fl}}_{\mathrm{geo}}(\xi)$

Geometry	$W^{\mathrm{fl}}_{\mathrm{geo}}(\xi)$	
2D circle, radius a	$\frac{1}{2\pi}\sum_{n=-\infty}^{\infty}\cos(n\theta)(f_n(\sigma_x r') - f_n(\sigma_m r'))$	(I05)
Finite cylinder, radius a, length l	$\frac{1}{\pi l}\sum_{k=1,\mathrm{odd}}^{\infty}\sum_{n=-\infty}^{\infty}\cos(n\theta)(f_n(\sigma_{zk} r') - f_n(\sigma_{mk} r'))$	(I06)
Infinite cylinder, radius a, $z = z'$	$\frac{1}{2\pi}\sum_{n=-\infty}^{\infty}\cos(n\theta)\sum_{\beta_n} g_n(\beta_n r')\left(\frac{1}{\sqrt{\sigma_x^2+\beta_n^2}} - \frac{1}{\sqrt{\sigma_m^2+\beta_n^2}}\right)$	(I07)
Sphere, radius a	$\frac{1}{4\pi\sqrt{qr'}}\sum_{n=0}^{\infty}\left(f_{n+\frac{1}{2}}(\sigma_x r') - f_{n+\frac{1}{2}}(\sigma_m r')\right)(2n+1)P_n(\cos\theta)$	(I08)
Note:	For all circular type geometries, such as the circle, cylinder, and sphere	
ZBC	$q = a, f_n(\varepsilon r') = \frac{1}{a}\frac{I_n(r'\varepsilon)}{I_n(a\varepsilon)}$, $g_n(\varepsilon r') = \frac{1}{a^2}\frac{J_n(r'\varepsilon)}{J_{n+1}(a\varepsilon)}$	
EBC	$q = b, f_n(\varepsilon r') = \frac{\varepsilon I_n(r'\varepsilon)}{I_n(b\varepsilon)}F'_n(a\varepsilon, b\varepsilon)$, $g_n(\varepsilon r') = \frac{1}{b^2}\frac{J'_n(a\varepsilon)J_n(r'\varepsilon)}{(J_{n+1}(b\varepsilon))^2}$	
	$F'_n(a\varepsilon, b\varepsilon) = \frac{-n}{a\varepsilon}F_n(a\varepsilon, b\varepsilon) - (I_{n-1}(a\varepsilon)K_n(b\varepsilon) + K_{n-1}(a\varepsilon)I_n(b\varepsilon))$	
	$F_n(a\varepsilon, b\varepsilon) = K_n(a\varepsilon)I_n(b\varepsilon) - I_n(a\varepsilon)K_n(b\varepsilon)$	

The Green's function for the infinite medium in spherical coordinates can be written as [12]

$$g^{\phi}_{\mathrm{inf}}(\mathbf{r}, \mathbf{r}', t, t') = \frac{e^{-\left(\mu_a c(t-t') + \frac{R^2}{4\gamma^2(t-t')}\right)}}{8\gamma\sqrt{\pi(t-t')}},$$

$$G^{\phi}_{\mathrm{inf}}(\mathbf{r}, \mathbf{r}', \omega, t') = \frac{e^{-j\omega(t-t')}e^{-\alpha R}}{2(2\pi)^{3/2}\gamma^2 R},$$

where $R^2 = r^2 + r'^2 - 2rr'\cos\theta$, in the time domain and the frequency domain, respectively.

By using an addition theorem in the Bessel function similar to earlier cases, G^{ϕ}_{inf} may be expressed as a form more suitable for spherical coordinates as $G^{\phi}_{\mathrm{inf}}(\mathbf{r}, \mathbf{r}', \omega, t') = (1/4\pi\gamma^2\sqrt{rr'})\sum_{n=0}^{\infty}(2n+1)I_{n+(1/2)}(\alpha r')K_{n+(1/2)}(\alpha r)P_n(\cos\theta)$ with $r > r'$. In case of $r < r'$, we interchange r and r' in the above expression. Imposing the condition $G^{\phi}_{\mathrm{inf}}(\mathbf{r}, \mathbf{r}', \omega, t') + H^{\phi}(\mathbf{r}, \omega) = 0$, we have $a_n = -(2n+1)((K_{n+(1/2)}(\alpha b) I_{n+(1/2)}(\alpha r'))/(4\pi\gamma^2\sqrt{r'}I_{n+(1/2)}(\alpha b)))$.

We proceed as in 2D circle case and arrive the following expressions for the Green's functions in the time and frequency domains, respectively:

$$\grave{g}^{\phi}_{\mathrm{sph}}(\mathbf{r}, \mathbf{r}', t, t') = \frac{e^{-\mu_a c(t-t')}}{2\pi b^2\sqrt{rr'}}\sum_{n=-\infty}^{\infty}\sum_{\beta_{n+\frac{1}{2}}} e^{-\gamma^2\beta^2_{n+\frac{1}{2}}(t-t')} \times \frac{J_{n+\frac{1}{2}}(\beta_{n+\frac{1}{2}}r)J_{n+\frac{1}{2}}(\beta_{n+\frac{1}{2}}r')}{\left(J'_{n+\frac{1}{2}}(\beta_{n+\frac{1}{2}}b)\right)^2} \times (2n+1)P_n(\cos\theta), \quad (77)$$

Table 8. Closed-form Expressions for Planar Type Geometries for Mean Time of Flight $\langle t^{\mathrm{fl}}_{\mathrm{geo}}\rangle(\xi) = \langle a^{\mathrm{fl}}_{\mathrm{geo}}\rangle(\xi) + (\tau + \zeta^2)$

Geometry	$\langle a^{\mathrm{fl}}_{\mathrm{geo}}\rangle(\xi)$	
Infinite	$\frac{1}{2}\frac{d^2\left(\frac{e^{-\sigma_x d}}{\gamma_x^2} - \frac{e^{-\sigma_m d}}{\gamma_m^2}\right)}{((1+\sigma_x d)e^{-\sigma_x d} - (1+\sigma_m d)e^{-\sigma_m d})}$	(t01)
Semi-infinite half-space	$\frac{1}{2}\frac{\frac{d_1}{\rho_1}\left(\frac{e^{-\sigma_x\rho_1}}{\upsilon_x} - \frac{e^{-\sigma_m\rho_1}}{\upsilon_m}\right) + \frac{d_2}{\rho_2}\left(\frac{e^{-\sigma_x\rho_2}}{\upsilon_x} - \frac{e^{-\sigma_m\rho_2}}{\upsilon_m}\right)}{\left[\frac{d_1}{\rho_1^3}((1+\sigma_x\rho_1)e^{-\sigma_x\rho_1} - (1+\sigma_m\rho_1)e^{-\sigma_m\rho_1}) + \frac{d_2}{\rho_2^3}((1+\sigma_x\rho_2)e^{-\sigma_x\rho_2} - (1+\sigma_m\rho_2)e^{-\sigma_m\rho_2})\right]}$	(t02)
ZBC	$d_1 = d_2 = z_0, \rho_1 = \rho_2 = \rho$	
EBC	$d_1 = z_0, d_2 = (z_0 + 2z_e), \rho_1 = \rho, \rho_2 = \grave{\rho}$	
Infinite slab $0 < z < d$ (at $z = d$)	$\frac{1}{2}\frac{\left[\sum_{n=0}^{\infty}\left\{\frac{d_1}{\rho_1}\left(\frac{e^{-\sigma_x\rho_1}}{\upsilon_x} - \frac{e^{-\sigma_m\rho_1}}{\upsilon_m}\right)\right\} - \sum_{n=0}^{\infty}\left\{\frac{d_2}{\rho_2}\left(\frac{e^{-\sigma_x\rho_2}}{\upsilon_x} - \frac{e^{-\sigma_m\rho_2}}{\upsilon_m}\right)\right\}\right]}{\left[\sum_{n=0}^{\infty}\left\{\frac{d_1}{\rho_1^3}((1+\sigma_x\rho_1)e^{-\sigma_x\rho_1} - (1+\sigma_m\rho_1)e^{-\sigma_m\rho_1})\right\} - \sum_{n=0}^{\infty}\left\{\frac{d_2}{\rho_2^3}((1+\sigma_x\rho_2)e^{-\sigma_x\rho_2} - (1+\sigma_m\rho_2)e^{-\sigma_m\rho_2})\right\}\right]}$	(t03)
ZBC	$d_1 = z_{+n}, d_2 = z_{-n}, \rho_1 = \rho_{+n}, \rho_2 = \rho_{-n}$	
EBC	$d_1 = \grave{z}_{+n}, d_2 = \grave{z}_{-n}, \rho_1 = \grave{\rho}_{+n}, \rho_2 = \grave{\rho}_{-n}$	
	Note: t' is implicitly assumed to be zero. It is easily verified that the correct result for $t' \neq 0$ is obtained by adding t' to $\langle t_{\mathrm{fl}}\rangle(\xi)$.	

Table 9. Closed-form Expressions for Various Geometries for Mean Time of Flight $\langle t_{\mathrm{geo}}^{\mathrm{fl}}\rangle(\xi) = \langle a_{\mathrm{geo}}^{\mathrm{fl}}(\xi)\rangle + (\tau + \zeta^2)$

Geometry	$\langle a_{\mathrm{geo}}^{\mathrm{fl}}\rangle(\xi)$
Infinite slab (at $z = 0$)	$\frac{1}{2}\frac{\mathcal{N}}{\mathcal{D}}$
	$\mathcal{N} = \frac{z_0}{\rho}\left(\frac{e^{-\sigma_x\rho}}{\upsilon_x} - \frac{e^{-\sigma_m\rho}}{\upsilon_m}\right) + \left[\sum_{n=0}^{\infty}\left\{\frac{d_1}{\rho_1}\left(\frac{e^{-\sigma_x\rho_1}}{\upsilon_x} - \frac{e^{-\sigma_m\rho_1}}{\upsilon_m}\right)\right\} - \sum_{n=0}^{\infty}\left\{\frac{d_2}{\rho_2}\left(\frac{e^{-\sigma_x\rho_2}}{\upsilon_x} - \frac{e^{-\sigma_m\rho_2}}{\upsilon_m}\right)\right\}\right]$
	$\mathcal{D} = \frac{z_0}{\rho^3}((1+\sigma_x\rho)e^{-\sigma_x\rho} - (1+\sigma_m\rho)e^{-\sigma_m\rho}) + \sum_{n=1}^{\infty}\frac{d_1}{\rho_1^3}((1+\sigma_x\rho_1)e^{-\sigma_x\rho_1} - (1+\sigma_m\rho_1)e^{-\sigma_m\rho_1})$
	$- \sum_{n=1}^{\infty}\frac{d_2}{\rho_2^3}((1+\sigma_x\rho_2)e^{-\sigma_x\rho_2} - (1+\sigma_m\rho_2)e^{-\sigma_m\rho_2})$ (t04)
ZBC	$d_1 = z_{+n'}$, $d_2 = z_{-n'}$, $\rho_1 = \rho_{+n'}$, $\rho_2 = \rho_{-n'}$
EBC	$d_1 = \dot{z}_{+n'}$, $d_2 = \dot{z}_{-n'}$, $\rho_1 = \dot{\rho}_{+n'}$, $\rho_2 = \dot{\rho}_{-n'}$
2D circle, radius a	$\frac{1}{2}\frac{\sum_{n=-\infty}^{\infty}\cos(n\theta)\left(\frac{1}{\upsilon_x}f'_n(\sigma_x r') - \frac{1}{\upsilon_m}f'_n(\sigma_m r')\right)}{\sum_{n=-\infty}^{\infty}\cos(n\theta)(f_n(\sigma_x r') - f_n(\sigma_m r'))}$ (t05)
Finite cylinder, radius a, length l	$\frac{\sum_{k=1,\mathrm{odd}}^{\infty}\sum_{n=-\infty}^{\infty}\cos(n\theta)\left(\frac{1}{\upsilon_{xk}}f'_n(\sigma_{xk} r') - \frac{1}{\upsilon_{mk}}f'_n(\sigma_{mk} r')\right)}{\sum_{k=1,\mathrm{odd}}^{\infty}\sum_{n=-\infty}^{\infty}\cos(n\theta)(f_n(\sigma_{xk} r') - f_n(\sigma_{mk} r'))}$ (t06)
Infinite cylinder, radius a, $z = z'$	$\frac{1}{2}\frac{\sum_{n=-\infty}^{\infty}\cos(n\theta)\sum_{\beta_n} g_n(\beta_n r')\left(\frac{1}{\gamma_x^2\sqrt{(\sigma_x^2+\beta_n^2)^3}} - \frac{1}{\gamma_m^2\sqrt{(\sigma_m^2+\beta_n^2)^3}}\right)}{\sum_{n=-\infty}^{\infty}\cos(n\theta)\sum_{\beta_n} g_n(\beta_n r')\left(\frac{1}{\sqrt{\sigma_x^2+\beta_n^2}} - \frac{1}{\sqrt{\sigma_m^2+\beta_n^2}}\right)}$ (t07)
	Note: t' is implicitly assumed to be zero. It is easily verified that the correct result for $t' \neq 0$ is obtained by adding t' to $\langle t_{\mathrm{fl}}\rangle(\xi)$.

Table 10. Closed-form Expressions for Circular Type Geometries for Mean Time of Flight $\langle t_{\mathrm{geo}}^{\mathrm{fl}}\rangle(\xi) = \langle a_{\mathrm{geo}}^{\mathrm{fl}}\rangle(\xi) + (\tau + \zeta^2)$

Geometry	$\langle a_{\mathrm{geo}}^{\mathrm{fl}}\rangle(\xi)$
Sphere, radius a	$\frac{1}{2}\frac{\sum_{n=0}^{\infty}\left(\frac{1}{\upsilon_x}f'_{n+\frac{1}{2}}(\sigma_x r') - \frac{1}{\upsilon_m}f'_{n+\frac{1}{2}}(\sigma_m r')\right)(2n+1)P_n(\cos\theta)}{\sum_{n=0}^{\infty}\left(f_{n+\frac{1}{2}}(\sigma_x r') - f_{n+\frac{1}{2}}(\sigma_m r')\right)(2n+1)P_n(\cos\theta)}$ (t08)
	Note: t' is implicitly assumed to be zero. It is easily verified that the correct result for $t' \neq 0$ is obtained by adding t' to $\langle t_{\mathrm{fl}}\rangle(\xi)$.
Note:	For all circular type geometries, such as the circle, cylinder, and sphere
ZBC	$q = a, f_n(\varepsilon r') = \frac{1}{a}\frac{I_n(r'\varepsilon)}{I_n(a\varepsilon)}$, $g_n(\varepsilon r') = \frac{1}{a^2}\frac{J_n(r'\varepsilon)}{J_{n+1}(a\varepsilon)}$, $f'_n(r'\varepsilon) = \frac{1}{a}\mathfrak{U}_n(\varepsilon r', a)$
EBC	$q = b, f_n(\varepsilon r') = \frac{\varepsilon I_n(r'\varepsilon)}{I_n(b\varepsilon)}F'_n(a\varepsilon, b\varepsilon)$, $g_n(\varepsilon r') = \frac{1}{b^2}\frac{J'_n(a\varepsilon)J_n(r'\varepsilon)}{(J_{n+1}(b\varepsilon))^2}$,
	$f'_n(r'\varepsilon) = (\frac{I_n(r'\varepsilon)}{I_n(b\varepsilon)} + \varepsilon\mathfrak{U}_n(\varepsilon r', b))F'_n(a\varepsilon, b\varepsilon) + \frac{\varepsilon I_n(r'\varepsilon)}{I_n(b\varepsilon)}\mathfrak{V}_n(\varepsilon a, \varepsilon b)$
	$\mathfrak{U}_n(r'\varepsilon, q) = \frac{r' I_n(q\varepsilon) I'_{n-1}(r'\varepsilon) - q I'_{n-1}(q\varepsilon) I_n(r'\varepsilon)}{(I_n(q\varepsilon))^2}$,
	$F'_n(a\varepsilon, b\varepsilon) = \frac{-n}{a\varepsilon}F_n(a\varepsilon, b\varepsilon) - (I_{n-1}(a\varepsilon)K_n(b\varepsilon) + K_{n-1}(a\varepsilon)I_n(b\varepsilon))$
	$\mathfrak{V}_n(a\varepsilon, b\varepsilon) = \left(\frac{n(2n+1)}{a\varepsilon^2} - a\right)F_n(a\varepsilon, b\varepsilon) + bF_{n-1}(a\varepsilon, b\varepsilon) + \frac{n-1}{\varepsilon}(I_{n-1}(a\varepsilon)K_n(b\varepsilon)$
	$+ K_{n-1}(a\varepsilon)I_n(b\varepsilon)) - \frac{bn}{a\varepsilon}(I_n(a\varepsilon)K_{n-1}(b\varepsilon) + K_n(a\varepsilon)I_{n-1}(b\varepsilon))$
	$F_n(a\varepsilon, b\varepsilon) = K_n(a\varepsilon)I_n(b\varepsilon) - I_n(a\varepsilon)K_n(b\varepsilon)$

$$\grave{G}^{\phi}_{\mathrm{sph}}(\mathbf{r},\mathbf{r}',\omega,t') = \frac{e^{-j\omega t'}}{2(2\pi)^{3/2}\gamma^2\sqrt{rr'}} \times \sum_{n=0}^{\infty} \frac{I_{n+\frac{1}{2}(r'\alpha)}}{I_{n+\frac{1}{2}(b\alpha)}} F_{n+\frac{1}{2}}(r\alpha, b\alpha) P_n(\cos\theta). \quad (78)$$

5. EXPRESSIONS FOR DIFFERENT DATA TYPES

The important measured quantities (data types) [5], which are of significance in the diffuse fluorescence spectroscopy/imaging, need to be evaluated, and the expressions for the same are listed as below.

(i) *Integrated intensity* (units: energy per unit area):

$$E_{\mathrm{fl}}(\xi) = \int_{-\infty}^{\infty} \Gamma_{\mathrm{fl}}(\xi, t)\mathrm{d}t, \quad (79)$$

where $\Gamma_{\mathrm{fl}}(\xi, t)$ is the temporal point-spread function (TSPF).

(ii) *Mean time of flight* (MTOF):

$$\langle t_{\mathrm{fl}}\rangle(\xi) = \frac{\int_{-\infty}^{\infty} t\Gamma_{\mathrm{fl}}(\xi, t)\mathrm{d}t}{\int_{-\infty}^{\infty} \Gamma_{\mathrm{fl}}(\xi, t)\mathrm{d}t}. \quad (80)$$

The expressions for $E_{\mathrm{fl}}(\xi)$ and $\langle t_{\mathrm{fl}}\rangle(\xi)$ for various geometries are derived as follows using the solutions listed in Tables 6–10. For any function $g(t)$ with $G(\omega)$ as its Fourier transform, one can write

$$\int_{-\infty}^{\infty} g(t)\mathrm{d}t = \sqrt{2\pi}G(\omega)|_{\omega=0} \quad \text{and,}$$
$$\frac{\partial}{\partial\omega}G(\omega) = \frac{1}{\sqrt{2\pi}}\frac{\partial}{\partial\omega}\int_{-\infty}^{\infty} g(t)e^{-j\omega t}\mathrm{d}t = -\frac{j}{\sqrt{2\pi}}\int_{-\infty}^{\infty} tg(t)\mathrm{d}t \quad (81)$$

and thus

$$\begin{aligned} E^{\mathrm{fl}}_{\mathrm{geo}}(\xi) &= \sqrt{2\pi}G^{\Gamma_{\mathrm{fl}}}(\omega)|_{\omega=0} \\ &= \frac{\sqrt{2\pi}n\zeta^2\gamma_m^2}{\gamma_m^2-\gamma_x^2}\left[G^{\Gamma_x}_{\mathrm{geo}}(\mathbf{r},\mathbf{r}',\omega,t') - G^{\Gamma_m}_{\mathrm{geo}}(\mathbf{r},\mathbf{r}',\omega,t')\right] \cdot \left[\frac{1}{\tau-\zeta^2}\left\{\frac{1}{\frac{1}{\tau}+j\omega} - \frac{1}{\frac{1}{\zeta^2}+j\omega}\right\}\right]\Bigg|_{\omega=0} \\ &= \frac{\sqrt{2\pi}n\zeta^2\gamma_m^2}{\gamma_m^2-\gamma_x^2}\left[G^{\Gamma_x}_{\mathrm{geo}}(\mathbf{r},\mathbf{r}',\omega,t') - G^{\Gamma_m}_{\mathrm{geo}}(\mathbf{r},\mathbf{r}',\omega,t')\right]\Big|_{\omega=0} \end{aligned} \quad (82)$$

Table 11. Glossary of Notation of Symbols Used in Tables 2–10

Symbol	Formula	Symbol	Formula
ξ	$=\sqrt{x^2+y^2}$	$\sigma_{x,m}$	$=\frac{\sqrt{\mu_{ax,am}c}}{\gamma_{x,m}}$
ρ	$=\sqrt{\xi^2+z_0^2}$	$\alpha_{x,m}$	$=\frac{\sqrt{\mu_{ax,am}c+j\omega}}{\gamma_{x,m}}$
z_{+n}	$=(2n+1)d+z_0$	$\alpha_{xk,mk}$	$=\left(\sqrt{\alpha_{x,m}^2+\frac{k^2\pi^2}{l^2}}\right)$
z_{-n}	$=(2n+1)d-z_0$	r'	Radial position of the source.
$z_{+n'}$	$=2nd+z_0$	β_j	Positive root of $J_j(\beta_j a)=0$, where $j=n,\ n+\frac{1}{2}$.
$z_{-n'}$	$=2nd-z_0$	ζ^2	$=\frac{\gamma_m^2-\gamma_x^2}{c(\gamma_m^2\mu_{ax}-\gamma_x^2\mu_{am})}$
$\grave{z}_{+n}$	$=(2n+1)(d+2z_e)+z_0$	$\grave{z}_{-n}$	$=(2n+1)(d+2z_e)-z_0$
$\grave{z}_{+n'}$	$=2n(d+2z_e)+z_0$	$\grave{z}_{-n'}$	$=2n(d+2z_e)-z_0$

Table 12. Glossary of Notation of Symbols Used in Tables 2–10

Symbol	Formula	Symbol	Formula
ρ_{+n}	$=\sqrt{\xi^2+z_{+n}^2}$	$v_{x,m}$	$=\gamma_{x,m}\sqrt{\mu_{ax,am}c}$
ρ_{-n}	$=\sqrt{\xi^2+z_{-n}^2}$	$\gamma_{x,m}$	$=\frac{c}{3(\mu_{ax,am}+\mu'_{sx,sm})}$
$\rho_{+n'}$	$=\sqrt{\xi^2+z_{+n'}^2}$	$\sigma_{xk,mk}$	$=\left(\sqrt{\frac{\mu_{ax,am}c}{\gamma_{x,m}^2}+\frac{k^2\pi^2}{l^2}}\right)$
$\rho_{-n'}$	$=\sqrt{\xi^2+z_{-n'}^2}$	$v_{xk,mk}$	$=\left(\sqrt{\mu_{ax,am}c+\frac{\gamma_{x,m}^2k^2\pi^2}{l^2}}\right)$
Bessel function	—	$J_\nu(x)$	$=\sum_{r=0}^{\infty}\frac{(-1)^r(\frac{1}{2}x)^{\nu+2r}}{r!\Gamma(\nu+r+1)}$
Modified Bessel function	—	$I_\nu(x)$	$=\sum_{r=0}^{\infty}\frac{(\frac{1}{2}x)^{\nu+2r}}{r!\Gamma(\nu+r+1)}$
Legendre polynomial	—	$P_n(x)$	$=\frac{1}{2^n n!}\frac{d^n}{dx^n}[(x^2-1)^n]$

$$\langle t_{\text{geo}}^{\text{fl}}\rangle(\xi) = j\frac{\frac{\partial}{\partial\omega}G^{\Gamma_{\text{fl}}}(\omega)\big|_{\omega=0}}{G^{\Gamma_{\text{fl}}}(\omega)\big|_{\omega=0}} = j\frac{\frac{\sqrt{2\pi}n\zeta^2\gamma_m^2}{\gamma_m^2-\gamma_x^2}\frac{\partial}{\partial\omega}\left\{\left(G_{\text{geo}}^{\Gamma_x}(\mathbf{r},\mathbf{r}',\omega,t') - G_{\text{geo}}^{\Gamma_m}(\mathbf{r},\mathbf{r}',\omega,t')\right)\cdot\left[\frac{1}{\tau-\zeta^2}\left(\frac{1}{\frac{1}{\tau}+j\omega}-\frac{1}{\frac{1}{\zeta^2}+j\omega}\right)\right]\right\}\Big|_{\omega=0}}{\frac{\sqrt{2\pi}n\zeta^2\gamma_m^2}{\gamma_m^2-\gamma_x^2}\left[G_{\text{geo}}^{\Gamma_x}(\mathbf{r},\mathbf{r}',\omega,t') - G_{\text{geo}}^{\Gamma_m}(\mathbf{r},\mathbf{r}',\omega,t')\right]\Big|_{\omega=0}}$$

$$= j\frac{\left[\frac{\partial}{\partial\omega}G_{\text{geo}}^{\Gamma_x}(\mathbf{r},\mathbf{r}',\omega,t') - \frac{\partial}{\partial\omega}G_{\text{geo}}^{\Gamma_m}(\mathbf{r},\mathbf{r}',\omega,t')\right]\Big|_{\omega=0}}{\left[G_{\text{geo}}^{\Gamma_x}(\mathbf{r},\mathbf{r}',\omega,t') - G_{\text{geo}}^{\Gamma_m}(\mathbf{r},\mathbf{r}',\omega,t')\right]\Big|_{\omega=0}} + (\tau+\zeta^2). \tag{83}$$

Note that the above equations are generic in nature; the specific solutions for various geometries are listed in Tables 6–10 with Tables 11 and 12 giving the glossary of terms used.

6. DISCUSSION AND CONCLUSIONS

Many closed-form Green's function solutions were proposed in the past for diffuse fluorescence spectroscopy/imaging in biological tissues, but they were dealing mostly with the infinite and semi-infinite geometries along with ZBCs [3,7–9]. Here, the usage of the EBC for various regular geometries (other than the infinite geometry) to derive generic Green's function solutions was attempted. A generic closed-form solution that could be used for any given geometry was derived, giving immense flexibility to obtain a solution for any kind of regular geometry. For example, the solution for the cube geometry, which is not discussed here, could easily be written using the heat equation solution as given in [12] (also shown in Section 2 of this work [10]).

Patterson and Pogue [3] have suggested (through Eq. (3) of [3]) that the general form of photon flux could be derived in the case of fluorescence imaging; here a formal derivation for various regular geometries using the first principles and Fourier transform techniques has been provided.

Assuming the fluorophore lifetime is negligibly small, i.e., $\tau = 0$ in Eqs. (5) and (6), leads to

$$q_{\text{fl}}(\mathbf{r},t) = \eta\mu_{af}N(\mathbf{r})\Phi_x(\mathbf{r},t), \tag{84}$$

$$Q_{\text{fl}}(\mathbf{r},\omega) = \eta\mu_{af}N(\mathbf{r})\Phi_x(\mathbf{r},\omega). \tag{85}$$

This case was extensively discussed by Sadoqi *et al.* [9], making the solution provided in [9] a special case of the closed-form solutions derived here.

Moreover, for the case of an EBC that closely mimics the real scenario, more than six geometries of closed-form expressions were derived in detail here. All expressions were derived using first principles without losing the generality. The comparison of the solutions obtained using zero and extrapolated boundary conditions and their validation has been taken up in the next part of the work [10]. Extension of the methods deployed here for irregular geometries and usage of these closed-form solutions to provide estimates of bulk (homogenous) fluorescence properties using the experimental data has also been discussed in the companion paper [10].

In summary, generic closed-form Green's function solutions for time- and frequency-domain diffuse fluorescence spectroscopy/imaging in biological tissues for the zero and extrapolated boundary cases have been derived in this work, and the expressions for various regular geometries have been provided for easy reference. The expressions for the derived data types, integrated intensity, and MTOF have been also been presented in this work.

ACKNOWLEDGMENTS

This work is supported by the Department of Atomic Energy Young Scientist Research Award (No. 2010/20/34/6/BRNS) by Government of India. The authors are grateful to the anonymous reviewers, who gave the idea of using EBCs, which improved the footage of the work presented here.

REFERENCES

1. M. A. Mycek and B. W. Pogue, eds., *Handbook of Biomedical Fluorescence* (Dekker, 2003).
2. E. M. Sevick-Muraca and J. C. Rasmussen, "Molecular imaging with optics: primer and case for near-infrared fluorescence techniques in personalized medicine," J. Biomed. Opt. **13**, 041303 (2008).
3. M. S. Patterson and B. W. Pogue, "Mathematical models for time-resolved and frequency-domain fluorescence spectroscopy in biological tissues," Appl. Opt. **33**, 1963–1974 (1994).
4. M. S. Patterson, B. Chance, and B. C. Wilson, "Time resolved reflectance and transmittance for the non-invasive measurement of tissue optical properties," Appl. Opt. **28**, 2331–2336 (1989).
5. S. R. Arridge, M. Cope, and D. T. Delpy, "The theoretical basis for the determination of optical path lengths in tissues: temporal and frequency analysis," Phys. Med. Biol. **37**, 1531–1560 (1992).
6. D. Contini, F. Martlli, and G. Zaccanti, "Photon migration through a turbid slab described by a model based on diffusion approximation. I. Theory, " Appl. Opt. **36**, 4587–4599 (1997).
7. M. A. O'Leary, D. A. Boas, B. Chance, and A. G. Yodh, "Reradiation and imaging of diffuse photon density waves using fluorescent inhomogeneities," J. Lumin. **60**, 281–286 (1994).
8. X. D. Li, B. Chance, and A. G. Yodh, "Fluorescent heterogeneities in turbid media: limits for detection, characterization, and comparison with absorption," Appl. Opt. **37**, 6833–6844 (1998).
9. M. Sadoqi, P. Riseborough, and S. Kumar, "Analytical models for time resolved fluorescence spectroscopy in tissues," Phys. Med. Biol. **46**, 2725–2743 (2001).
10. K. R. Ayyalasomayajula and P. K. Yalavarthy, "Analytical solutions for diffuse fluorescence spectroscopy/imaging in biological tissues Part II: comparison and validation," J. Opt. Soc. Am. A **30**, 553–559 (2013).
11. J. W. Brown and R. V. Churchill, *Complex Variables and Applications*, 7th ed. (McGraw-Hill, 2004).
12. H. S. Carslaw and J. C. Jaeger, *Conduction of Heat in Solids*, 2nd ed. (Oxford Science, 1946).
13. G. N. Watson, *A Treatise on the Theory of Bessel Functions*, 2nd ed. (Cambridge University, 1992).
14. A. Gray and G. B. Mathews, *A Treatise on Bessel Functions and Their Applications to Physics* (Macmillan, 1895).